Cell Systems

Brief report

Concentration buffering and noise reduction in non-equilibrium phase-separating systems

Highlights

- Concentration buffering and noise reduction are often not clearly distinguished
- We show that these phenomena are distinct in non-equilibrium conditions
- A fixed saturation concentration is not required for effective noise reduction
- Inference of solute interactions using equilibrium phase diagrams is unreliable in cells

Authors

Christoph Zechner, Frank Jülicher

Correspondence

czechner@sissa.it (C.Z.), julicher@pks.mpg.de (F.J.)

In brief

Phase-separated compartments have been demonstrated to reduce cellular noise. This idea has been challenged in multicomponent systems, where concentrations need not be buffered when individual components are varied. Here, we show that concentration buffering and noise reduction are distinct concepts and that one cannot be inferred from the other.

Zechner & Jülicher, 2025, Cell Systems *16*, 101168
February 19, 2025
https://doi.org/10.1016/j.cels.2025.101168

CellPress

Please cite this article in press as: Zechner and Jülicher, Concentration buffering and noise reduction in non-equilibrium phase-separating systems, Cell Systems (2025), https://doi.org/10.1016/j.cels.2025.101168

Cell Systems

CellPress
OPEN ACCESS

Brief report

Concentration buffering and noise reduction in non-equilibrium phase-separating systems

Christoph Zechner[1,2,4,5,6,7,*] and Frank Jülicher[1,3,4,*]
[1]Center for Systems Biology Dresden, Dresden, Germany
[2]Max Planck Institute of Molecular Cell Biology and Genetics, Dresden, Germany
[3]Max Planck Institute for the Physics of Complex Systems, Dresden, Germany
[4]Cluster of Excellence Physics of Life, TU Dresden, Dresden, Germany
[5]Faculty of Computer Science, TU Dresden, Dresden, Germany
[6]Present address: Scuola Internazionale Superiore di Studi Avanzati, Trieste, Italy
[7]Lead contact
*Correspondence: czechner@sissa.it (C.Z.), julicher@pks.mpg.de (F.J.)
https://doi.org/10.1016/j.cels.2025.101168

SUMMARY

Biomolecular condensates have been proposed to buffer intracellular concentrations and reduce noise. However, concentrations need not be buffered in multicomponent systems, leading to a non-constant saturation concentration (c_{sat}) when individual components are varied. Simplified equilibrium considerations suggest that noise reduction might be closely related to concentration buffering and that a fixed saturation concentration is required for noise reduction to be effective. Here, we present a theoretical analysis to demonstrate that these suggestions do not apply to mesoscopic fluctuating systems. We show that concentration buffering and noise reduction are distinct concepts, which cannot be used interchangeably. We further demonstrate that concentration buffering and a constant c_{sat} are neither necessary nor sufficient for noise reduction to be effective. Clarity about these concepts is important for studying the role of condensates in controlling cellular noise and for the interpretation of concentration relationships in cells. A record of this paper's transparent peer review process is included in the supplemental information.

INTRODUCTION

Biomolecular condensates are membraneless compartments that are segregated from the surrounding cytoplasm by phase coexistence.[1] The thermodynamic constraints of coexisting phases restrict the potential concentration ranges of multicomponent mixtures.[2–8] This opens the possibility for cells to regulate concentrations by condensate formation. An important question is how such physical processes can be utilized to control fluctuations and molecular noise.[1,9,10]

We have previously demonstrated noise reduction by condensates theoretically as well as experimentally using engineered and endogenous systems.[11] Others have observed that the coexisting concentrations of certain intracellular condensates are not buffered when individual components are overexpressed.[7] In other words, they do not exhibit a fixed saturation concentration c_{sat}.[7] Some studies have considered concentration buffering and noise reduction as interchangeable,[7,12,13] suggesting that the absence of a fixed saturation concentration hampers noise reduction. However, noise reduction has been demonstrated for an endogenously labeled component of the nucleolus,[11] an intracellular condensate lacking a fixed saturation concentration.[7] This raises the question in what situations do noise reduction and concentration buffering become related and when these phenomena are clearly distinct.

Here, we provide precise definitions of the concepts of concentration buffering and noise reduction and clarify if and how they relate to each other. Since intracellular condensates are exposed to active fluctuations, we develop a non-equilibrium theory of multicomponent systems, which captures the stochastic kinetics of material production and turnover, as well as exchange between phases. Our analysis shows that concentration buffering and noise reduction are distinct phenomena and that a fixed c_{sat} is neither necessary nor sufficient for noise reduction to take place. This becomes particularly important in non-equilibrium conditions such as those found in the cell. To illustrate our findings, we will discuss them in the context of previously published data from synthetic and endogenous condensates in cells.[7,11]

RESULTS AND DISCUSSION

Concentration buffering

We consider a multicomponent system with two coexisting phases that differ in the concentrations of their components (Figure 1A). We focus on one component A that partitions between the two phases and denote by c the total average concentration $c = a/V$, i.e., the total copy number of molecules a per volume V of both phases combined. The concentrations of the same component in the coexisting phases are referred to as c_1 and

Please cite this article in press as: Zechner and Jülicher, Concentration buffering and noise reduction in non-equilibrium phase-separating systems, Cell Systems (2025), https://doi.org/10.1016/j.cels.2025.101168

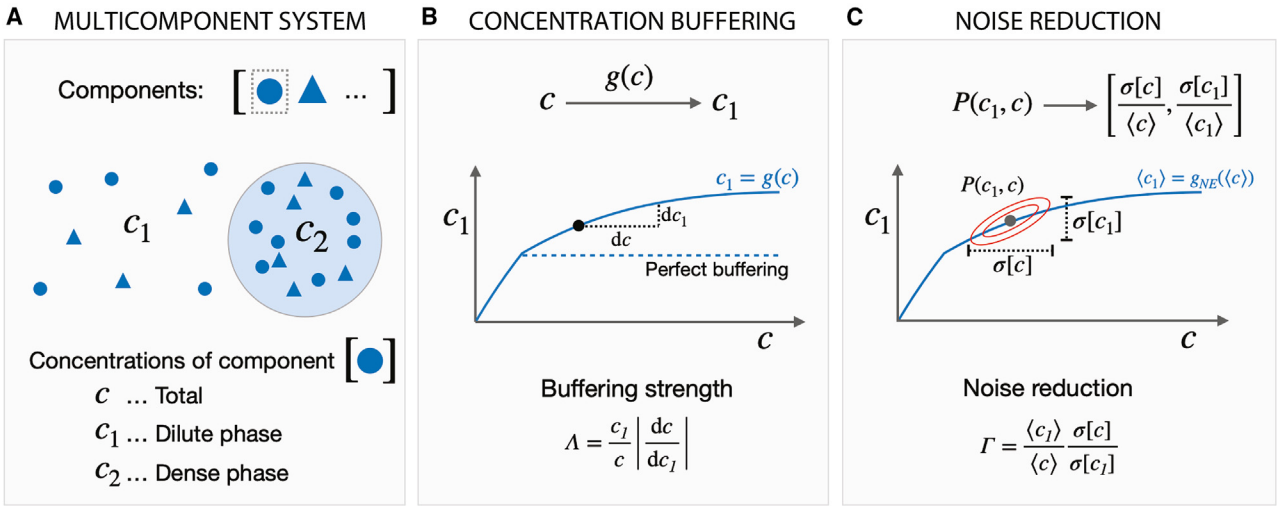

Figure 1. Concentration buffering and noise reduction in phase-separating systems

(A) Scheme of a multicomponent system with two coexisting phases. Symbols c, c_1, and c_2 denote total-, dilute-, and dense phase concentrations of the considered component A.

(B) Concentration buffering in the dilute phase can be quantified by the buffering strength Λ, which we define as the inverse relative sensitivity of the dilute phase concentration $c_1 = g(c)$ with respect to changes in total concentration c, or equivalently, $\Lambda = \mathrm{d}\log c/\mathrm{d}\log c_1$.

(C) Noise reduction Γ can be defined as the ratio of the relative variabilities $\sigma[.]/\langle.\rangle$ in total- and dilute phase concentration.

c_2, respectively. We refer to c_1 and c_2 as dilute- and dense phase concentration, where $c_2 > c_1$. The partitioning of the component A is generally composition-dependent, and therefore, c_1 and c_2 depend on c and on the total concentrations of all other components. In the following, we focus on the relationship between dilute phase concentration c_1 and total concentration c and consider the total concentrations of all other components to be fixed. When the system is in thermodynamic equilibrium and taking the thermodynamic limit, the dilute phase concentration c_1 is described by the binodal manifold in a multicomponent phase diagram. It can be formally expressed as a unique function $c_1 = g(c)$ of composition where we omit the constant concentrations of all other components. In the following, we refer to function g as concentration dependence. Concentration buffering of the dilute phase concentration c_1 occurs when g is insensitive to changes in c (Box 1). To quantify concentration buffering, we define the buffering strength in the dilute phase

$$\Lambda = \left|\frac{\mathrm{d}\log c_1}{\mathrm{d}\log c}\right|^{-1} = \frac{1}{c}\frac{g(c)}{|g'(c)|}, \qquad \text{(Equation 1)}$$

where g' denotes the derivative of g with respect to c (Figure 1B). The buffering strength measures the logarithmic sensitivity of the dilute phase concentration c_1 with respect to changes in total concentration c. We take the inverse to ensure that low sensitivities correspond to large buffering strengths. The logarithms imply that relative changes are considered. In a binary mixture at equilibrium with segregated macroscopic phases, c_1 is constant when c increases, i.e., $g' = 0$ and the buffering strength Λ formally diverges. In this singular case, c_1 is perfectly buffered as it is constrained to a fixed saturation concentration c_{sat} in the two-phase regime. In general, however, the buffering strength is a finite positive number, capturing how strongly c_1 varies with c. As an example, a buffering strength of $\Lambda = 10$ implies that when c changes by 10%, then c_1 changes by only 1%. Even though the saturation concentration in this system is not fixed, the dilute phase concentration c_1 is buffered effectively. The buffering strength can be generalized to non-equilibrium steady states where g becomes a non-equilibrium concentration dependence g_{NE}. As we will discuss below, concentration buffering is often reduced in non-equilibrium conditions.

Noise reduction

We now consider a phase-separating system exhibiting concentration fluctuations, which we refer to as noise. The presence of noise renders both quantities, the total concentration c and the dilute phase concentration c_1 time-dependent. Moreover, the relationship between c and c_1 becomes stochastic as captured by the joint probability distribution $P(c, c_1)$. In the following, we consider the case where the statistics of the noise are stationary. In order to quantify noise reduction, we compare the probability distribution over total concentration $P(c) = \int P(c_1, c)dc_1$ to the probability distribution over dilute phase concentration $P(c_1) = \int P(c_1, c)dc$ (Figure 1C and Box 1). A common dimensionless measure for the magnitude of noise is the coefficient of variation $\eta[x] = \sigma[x]/\langle x\rangle$, where $\sigma[x]$ and $\langle x\rangle$ are the standard deviation and mean of random variable x, respectively. The coefficient of variation measures the variability of x relative to its mean, which is useful when comparing quantities of different magnitude. Noise reduction in the dilute phase can then be defined as the ratio of coefficients of variation of total- and dilute phase concentration

$$\Gamma = \frac{\eta[c]}{\eta[c_1]} = \frac{\sigma[c]}{\sigma[c_1]}\frac{\langle c_1\rangle}{\langle c\rangle}, \qquad \text{(Equation 2)}$$

such that noise is reduced when $\Gamma > 1$ and $\eta[c_1] < \eta[c]$.

Please cite this article in press as: Zechner and Jülicher, Concentration buffering and noise reduction in non-equilibrium phase-separating systems, Cell Systems (2025), https://doi.org/10.1016/j.cels.2025.101168

CellPress
OPEN ACCESS

Box 1. Definition of concentration buffering and noise reduction

Concentration buffering is the maintenance of concentration near a set value even if material is added or removed. In phase-separating systems, concentration buffering may occur in both two- and multicomponent systems. Two-component systems at equilibrium can exhibit a fixed saturation concentration c_{sat}, that is, the dilute phase concentration c_1 remains virtually constant at different total concentrations c. Multicomponent systems exhibit saturation concentrations that depend on the concentration of all components. Therefore, multicomponent systems may show limited concentration buffering at equilibrium. In non-equilibrium conditions, new behaviors can arise and even two-component systems may not exhibit a fixed c_{sat}. However, systems lacking a fixed c_{sat} may still achieve substantial concentration buffering. In noisy systems, concentration buffering may be defined using average concentrations $\langle c\rangle$ and $\langle c_1\rangle$ because concentrations fluctuate.

Noise reduction is a decrease of the variability of random fluctuations around an average. A phase-separating system exhibits noise reduction in the dilute phase when fluctuations in the dilute phase concentration c_1 are smaller than fluctuations in the total concentration c. Fluctuations can be quantified by the coefficient of variation $\eta[.] = \sigma[.]/\langle.\rangle$, which is suitable for comparing fluctuations of a random variable around its average. Noise reduction is different from concentration buffering. In a phase-separating system, noise reduction is not directly linked to the existence of a fixed saturation concentration c_{sat}. Conversely, if the average dilute phase concentration is buffered, noise is not necessarily reduced. In non-equilibrium systems, noise reduction depends on the timescales of the underlying kinetic processes.

Molecular noise in cells is dynamic and spans a spectrum of timescales, ranging over orders of magnitude.[14–16] How fluctuations at different timescales are affected by a system depends on how the timescales of the noise compare to the intrinsic timescales of that system. As an example, a system may effectively suppress low-frequency fluctuations but fail to suppress or even amplify high-frequency fluctuations. Similar to the buffering strength, noise reduction is a quantitative property. In cells, a reduction of noise by a factor of as little as $1.5 - 2$ can already be substantial and require high metabolic cost when realized through active biochemical feedback.[17,18]

Concentration buffering and noise reduction are distinct phenomena

Simple considerations suggest that concentration buffering and noise reduction may be closely related concepts.[2,7,12,13] This viewpoint originates from the idea that when c_1 is insensitive to c (perfect buffering, $\Lambda \to \infty$), it should buffer variations in c and leave c_1 more or less unaffected even if c fluctuates. Comparing concentration buffering and noise reduction more closely, however, reveals that they are different and cannot be used synonymously. In general, concentration buffering cannot be used to predict noise reduction, nor can it provide bounds on it as we will show below.

To better understand this, it is useful to first address the question under what special conditions concentration buffering and noise reduction do become similar. Consider an ensemble of equilibrium systems, each being at the thermodynamic limit with concentration relationship $g(c)$. The systems only differ in the total concentrations c, which are randomly distributed according to a probability distribution $P(c)$. Physically, this corresponds to an equilibrium ensemble or to a quasi-static system, where the composition changes slowly compared with the relaxation to equilibrium. Since c varies, also c_1 varies across the ensemble according to some probability distribution $P(c_1)$. If we consider small variations around the average total concentration $\langle c\rangle$, the standard deviation of c_1 becomes $\sigma[c_1] \simeq \sigma[c]|g'(\langle c\rangle)|$. Using this expression in the definition of noise reduction (Equation 2) yields

$$\Gamma = \frac{1}{\langle c\rangle}\frac{g(\langle c\rangle)}{|g'(\langle c\rangle)|} \qquad \text{(Equation 3)}$$

which is identical to the buffering strength (Equation 1) evaluated at the average total concentration $\langle c\rangle$. In other words, concentration buffering and noise reduction become similar for large equilibrium systems with slowly fluctuating composition. Note, however, that this special case entails a strong simplification of the concept of noise reduction, essentially reducing it to the transformation of the random variable c by a static nonlinearity g.

In the cell biological context, molecular noise is discussed in the context of mesoscopic stochastic systems, whose degrees of freedom fluctuate dynamically and which are out of equilibrium. While noise reduction as defined in Equation 2 is well defined for such systems, the buffering strength defined in Equation 1 needs to be reconsidered. This is because the total- and dilute phase concentrations are random variables, whose relationship cannot be expressed by a deterministic function. Alternatively, we can define the relationship between average concentrations $\langle c_1\rangle = g_{NE}(\langle c\rangle)$ and use this function g_{NE} instead of g in the definition of the buffering strength in Equation 1. However, concentration buffering then becomes a property of average concentrations, while noise reduction is concerned with fluctuations around such averages. In general, these two quantities provide different information. In the following, we will use theory and numerical analyses to probe the relationship between concentration buffering and noise reduction in mesoscopic phase-separating systems away from equilibrium.

Stochastic dynamics of phase-separating systems in the presence of active synthesis and turnover of molecules

We consider a three-component mixture consisting of two solutes A and B and solvent S. While mixtures comprising more than three components could be handled analogously, a ternary mixture is sufficient for the following discussion. The copy numbers of the components are denoted by a, b and s, respectively. The solvent S is associated with a molecular volume v, while the two solutes A and B are considered to have equal molecular volume $v_A = v_B = nv$ for simplicity. We describe the composition of the mixture using volume fractions $\phi = av_A/V$ and $\psi = bv_B/V$, which are particle concentrations multiplied by the respective molecular volumes v_A and v_B. We denote the

Please cite this article in press as: Zechner and Jülicher, Concentration buffering and noise reduction in non-equilibrium phase-separating systems, Cell Systems (2025), https://doi.org/10.1016/j.cels.2025.101168

volume fractions of solute molecules in the dilute- and dense phase as $\phi_\alpha = v_A a_\alpha / V_\alpha$ and $\psi_\alpha = v_B b_\alpha / V_\alpha$ for $\alpha \in \{1,2\}$, respectively. Since volume fractions can be understood as rescaled concentrations, we will refer to them as concentrations in the following to simplify terminology. At equilibrium, this system can be described by a free energy

$$F = V_1 f(\phi_1, \psi_1) + V_2 f(\phi_2, \psi_2) + \gamma \mathcal{A}_2 \qquad \text{(Equation 4)}$$

with f as a ternary Flory-Huggins free energy density,[19,20] γ the surface tension, V_1 and V_2 denoting the volumes of dilute and dense phase and $\mathcal{A}_2 \sim V_2^{2/3}$ as the surface area of the dense phase. The free energy density f is governed by three effective interaction parameters χ_{AS}, χ_{BS} and χ_{AB} capturing effects of pairwise interactions among A, B, and S. Considering incompressibility ($V = V_1 + V_2 = const.$) and conserved copy numbers a and b, the system can be described by three degrees of freedom, e.g., the dilute phase copy numbers a_1, b_1, and s_1. The dependencies of dilute phase concentration on total concentration at equilibrium can be obtained by minimizing the free energy (Equation 4) with respect to a_1, b_1, and s_1 (STAR Methods section "Equilibrium theory").

In the presence of molecular synthesis and degradation, the solute copy numbers a and b are no longer conserved. In this case, a, b, and also a_1, b_1, and s_1 are stochastic degrees of freedom. We describe copy-number fluctuations of a and b using birth-and-death processes with fluctuating birth-rate.[21] In case of a, for instance, we consider a stochastic time-dependent birth-rate $V k_1^A r_A(t)$ with rate constant k_1^A and a dimensionless stochastic process $r_A(t)$. The process $r_A(t)$ can account for additional sources of randomness affecting the synthesis of components A such as fluctuations in the number of messenger RNA or extrinsic sources of variability.[21,22] We consider $r_A(t)$ to be at stationarity with mean $\langle r_A \rangle$ and autocovariance function $\kappa_A(\tau) = \langle r_A(t) r_A(t+\tau) \rangle - \langle r_A \rangle^2$, where τ is the lag time. Degradation of molecules A takes place with rate $k_2 a(t)$, where $1/k_2$ is the average lifetime of a molecule. For simplicity, the same birth- and degradation rates are used in both phases. We can now calculate the mean and the variance of total concentration ϕ of solute A. The resulting stationary noise strength of total concentration ϕ reads

$$\eta^2[\phi] = \frac{1}{V} \frac{k_2}{k_1^A \langle r_A \rangle} + \frac{k_2}{\langle r_A \rangle^2} \widehat{\kappa}_A(k_2) \qquad \text{(Equation 5)}$$

where $\widehat{\kappa}_A(u)$ is the Laplace transform of the autocovariance function $\kappa_A(\tau)$, which in Equation 5 is evaluated at the degradation rate $u = k_2$ (STAR Methods section "Accounting for non-equilibrium production and turnover of solutes"). Fluctuations of the second solute B are treated analogously. To study how fluctuations in total concentration relate to fluctuations in the dilute (or dense) phase, we have to account for the kinetics of material exchange between phases. Specifically, we consider diffusion-limited exchange of solutes between dilute- and dense phase as well as rapid relaxation of solvent to osmotic equilibrium. The kinetics of these events are governed by differences in chemical potentials, involving osmotic pressure and Laplace pressure (STAR Methods sections "Kinetics of solute and solvent partitioning" and "Droplet kinetics in the presence of non-equilibrium production and turnover of solutes"). The statistical properties of this system can be described by a master equation, which we solve numerically using the linear noise approximation.[23] The resulting statistics allow us to analyze both noise reduction and concentration buffering for components A and B in non-equilibrium conditions (STAR Methods section "Droplet kinetics in the presence of non-equilibrium production and turnover of solutes").

Non-equilibrium systems lack fixed saturation concentrations

We first consider concentration buffering and noise reduction in a simple binary mixture with only solute A and solvent S (no component B, $\psi = 0$). Attractive interactions among solute molecules A or repulsive interactions between A and S are captured by a single interaction parameter $\chi_{AS} > 0$. The total concentration ϕ of solutes A fluctuates due to synthesis and turnover as specified above. The stochastic process $r_A(t)$ is chosen to be a birth-and-death process with birth-rate λ_1 and death-rate $\lambda_2 r_A(t)$ mimicking for example stochastic synthesis and degradation of messenger RNA. The stationary mean and autocovariance function of $r_A(t)$ are then given by $\langle r_A \rangle = \lambda_1/\lambda_2$ and $\kappa_A(\tau) = \lambda_1/\lambda_2 e^{-\lambda_2 \tau}$.

To study concentration buffering in this system, we determine the dependence of the average dilute phase concentration on total concentration, $\langle \phi_1 \rangle = g_{NE}(\langle \phi \rangle)$ and compare it to the dilute phase concentration at equilibrium $\phi_1 = g(\phi)$. For a phase-separated two-component system at equilibrium, we have $g(\phi) \simeq \phi_{sat}$, where ϕ_{sat} is the equilibrium saturation concentration in the thermodynamic limit (Figure 2A, black line). This is no longer the case in non-equilibrium conditions, where $\langle \phi_1 \rangle = g_{NE}(\langle \phi \rangle)$ increases with average total concentration $\langle \phi \rangle$ (Figures 2A blue line and S1). For the considered two-component system, approximate expressions can be derived if dilute phase concentrations ϕ_1 and droplet volumes V_2 are small (dilute approximation; see STAR Methods section "Analytical results for the case of a two-component mixture"). In the two-phase regime, $g_{NE}(\langle \phi \rangle)$ is given by

$$g_{NE}(\langle \phi \rangle) \simeq \frac{k_D}{k_2 + k_D} \phi_{sat} + \frac{k_2}{k_2 + k_D} \langle \phi \rangle \qquad \text{(Equation 6)}$$

where $k_D \sim D/V^{2/3}$ is a kinetic coefficient that captures the diffusion-limited exchange of molecules between dilute- and dense phase with diffusion constant D. Equation 6 demonstrates that the slope of $g_{NE}(\langle \phi \rangle)$ depends on the relative timescale between molecular turnover and partitioning, whereas perfect concentration buffering ($\langle \phi_1 \rangle \to \phi_{sat}$) is reached only when k_D is much larger than the degradation rate k_2 and the phases reach equilibrium. At finite degradation rate, the two phases cannot equilibrate during the characteristic time of diffusion. Because the dilute phase concentration is not fixed, the apparent partition coefficient, which we define as $\rho = \langle \phi_2 \rangle / \langle \phi_1 \rangle$ is also not constant but decreases with increasing $\langle \phi \rangle$, i.e.,

$$\rho = \frac{\tilde{\phi}_2 (k_2 + k_D)}{\phi_{sat} k_D + k_2 \langle \phi \rangle} \qquad \text{(Equation 7)}$$

Please cite this article in press as: Zechner and Jülicher, Concentration buffering and noise reduction in non-equilibrium phase-separating systems, Cell Systems (2025), https://doi.org/10.1016/j.cels.2025.101168

CellPress
OPEN ACCESS

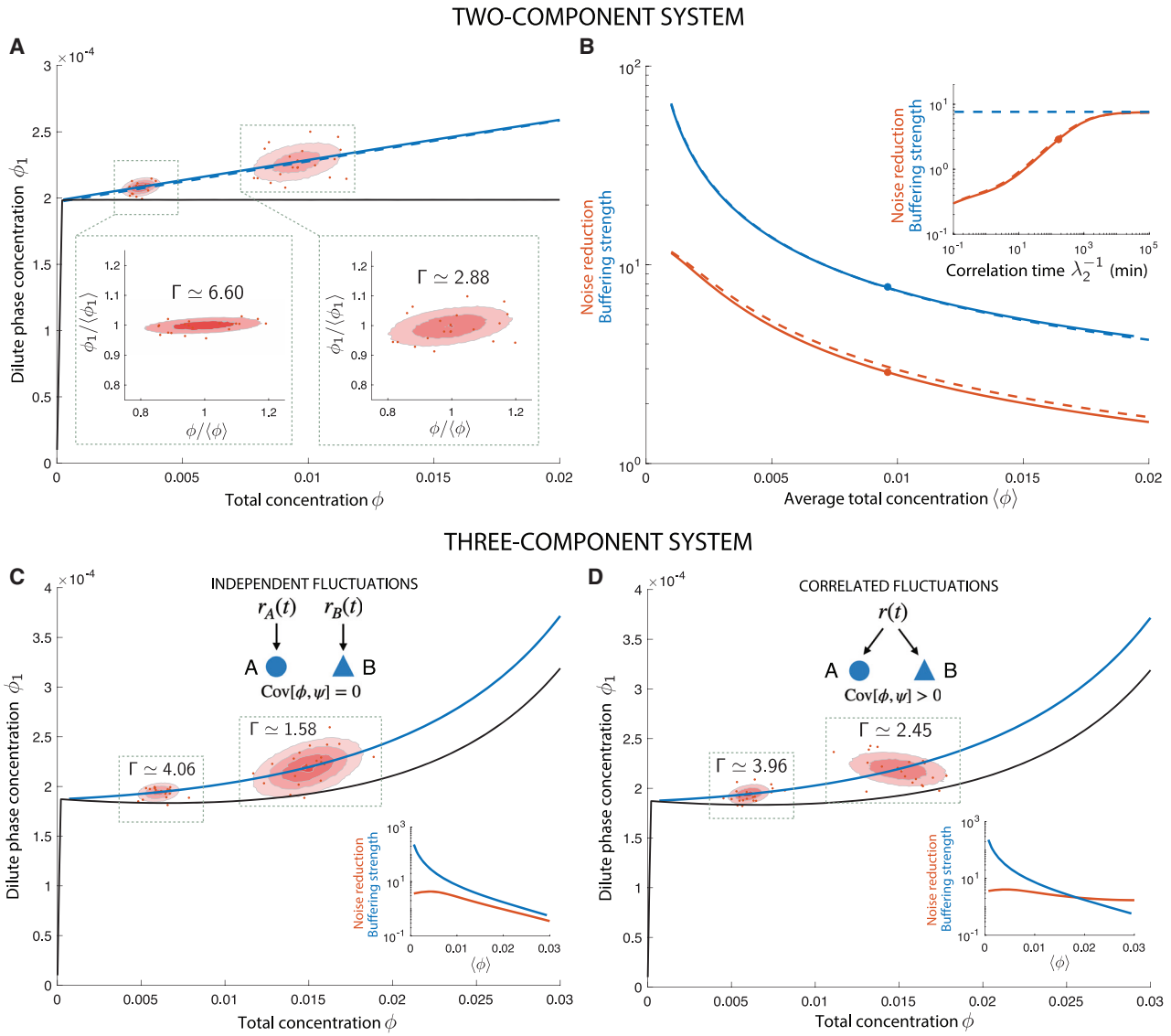

Figure 2. Concentration buffering and noise reduction out of equilibrium

(A and B) Two-component system consisting of a solute *A* and solvent *S*. The total concentration of *A* is described by $\phi = cv_A$. (A) Dilute phase concentration ϕ_1 as a function of total concentration ϕ of solute *A*. Joint distributions over total- and dilute phase concentrations are illustrated as ellipses for two different average total concentrations. Representative samples are shown as red dots. Insets show distributions over relative concentrations $\phi/\langle\phi\rangle$ and $\phi_1/\langle\phi_1\rangle$, illustrating relative variability of ϕ and ϕ_1, respectively.

(B) Comparison between buffering strength (blue) and noise reduction (red). The buffering strength and noise reduction under the dilute approximation are shown as dashed lines. Inset: buffering strength and noise reduction for varying correlation times $1/\lambda_2$ of the process $r_A(t)$.

(C and D) Three-component system consisting of solutes *A* and *B* and solvent *S*. (C) Fluctuations in *A* and *B* are independent. (D) Fluctuations in *A* and *B* are correlated. Insets: buffering strength and noise reduction for varying $\langle\phi\rangle$. Black lines correspond to systems at equilibrium. Parameter values are provided in Tables S1–S3.

where $\tilde{\phi}_2$ denotes the average dense phase concentration that is approximately constant (STAR Methods section "Analytical results for the case of a two-component mixture"). Even when solute partitioning is around $2-3$ orders of magnitude faster than solute turnover, the apparent partition coefficient and average dilute phase concentration change substantially with average total concentration (Figure S1). Thus, while a fixed saturation concentration and partition coefficient are hallmarks of binary systems at equilibrium,[7,12,24] these features are lost in non-equilibrium steady states where material is subject to production and turnover.

To compare these results with experiments, we used previously published data on the synthetic model protein 2NT-DDX4^{YFP}.[11] The 2NT-DDX4^{YFP} construct was overexpressed in cells, which generated large variability in expression levels below and above the phase-separation threshold. Condensates began to form at

Please cite this article in press as: Zechner and Jülicher, Concentration buffering and noise reduction in non-equilibrium phase-separating systems, Cell Systems (2025), https://doi.org/10.1016/j.cels.2025.101168

around 7 μM, but average dilute phase concentrations did not remain constant but tended to increase with average total concentration (Figure S2A). Fitting Equation 6 to the data, revealed a slope of $k_2/(k_2+k_D) \simeq 0.04$, corresponding to a case where protein partitioning is around 20 times faster than turnover (STAR Methods section "Synthetic system"). We further display the partition coefficient for a smaller dataset from the same study,[11] where both dilute- and dense phase concentrations were measured, revealing that the partition coefficient decreases for increasing dilute phase concentration and hence total concentration (Figure S2A, inset). Variable dilute phase concentrations and partition coefficients have been previously associated with condensates that rely on heterotypic interactions.[7] While we do not exclude a potential role of heterotypic interactions in the 2NT-DDX4^{YFP} condensate, its variable average dilute phase concentration and partition coefficient are consistent even with a binary system with molecular synthesis and turnover. Therefore, from observed variable compositions or partition coefficients in a cell, one cannot infer that heterotypic interactions drive condensate formation, in contrast to previous suggestions.[5,7,24]

A fixed saturation concentration is not required for effective concentration buffering and noise reduction

We next analyzed how the absence of a fixed saturation concentration affects concentration buffering and the reduction of noise. To this end, we determined the buffering strength and noise reduction of the non-equilibrium binary system for different average total concentrations $\langle\phi\rangle$ (Figures 2A and 2B). Both the buffering strength and noise reduction decrease with increasing average total concentration $\langle\phi\rangle$, ranging from about 60- to 5- and 10- to 2-fold, respectively (Figure 2B, blue and red lines). This demonstrates that both quantities depend strongly on the systems' setpoint $\langle\phi\rangle$ and that they can attain very large values even when the average dilute phase concentration $\langle\phi_1\rangle$ varies strongly.

This analysis further reveals that the buffering strength and noise reduction can assume substantially different values for a given average total concentration $\langle\phi\rangle$ (Figure 2B). To better understand this difference, we make use of the dilute approximation (STAR Methods section "Analytical results for the case of a two-component mixture"), for which the buffering strength is

$$\Lambda = 1+\frac{k_D}{k_2}\frac{\phi_{sat}}{\langle\phi\rangle} \qquad \text{(Equation 8)}$$

Noise reduction, by contrast takes a more complex form $\Gamma = \eta[\phi]/\eta[\phi_1]$ with $\eta[\phi] = \sqrt{\eta^2[\phi]}$ given by Equation 5 and

$$\eta[\phi_1] = \sqrt{\frac{nv}{V\langle\phi_1\rangle}+\frac{1}{k_2+k_D}\left(\frac{k_1^A nv}{\langle\phi_1\rangle}\right)^2\widehat{\kappa}_A(k_2+k_D)} \qquad \text{(Equation 9)}$$

with $\langle\phi_1\rangle = g_{NE}(\langle\phi\rangle)$ as defined in Equation 6 (STAR Methods section "Analytical results for the case of a two-component mixture"). Comparing the buffering strength with noise reduction, we realize that the latter depends on the correlation function $\widehat{\kappa}_A$ and the system size V, while the former does not. The size-dependence of noise reduction originates from intrinsic fluctuations of solute partitioning, synthesis, and turnover. The dependence on $\widehat{\kappa}_A$ captures how temporal fluctuations of the birth-rate r_A propagate to ϕ and ϕ_1, respectively. Noise reduction becomes similar to the buffering strength in the limit of both large systems ($V\to\infty$) and long correlation time of the birth-rate r_A ($\lambda_2\to 0$) while keeping k_D fixed (STAR Methods section "Noise reduction in the limit of large volumes and quasi-static birth-rates"). However, cells do not typically operate close to these limits.[14,22,25–27] As an example, in Figure 2B, we consider r_A to have a correlation time of $1/\lambda_2 \simeq 3h$ (e.g., due to transcriptional fluctuations[15] or mRNA decay[28]) together with a solute lifetime of $1/k_2 \simeq 14$ h[28,29] and a partitioning time of $1/k_D \simeq 2.6$ min. The latter is comparable to the timescales observed in cells.[11,30,31] Using $k_D = 6D/V^{2/3}$, this corresponds to e.g., $D \simeq 0.2\,\mu\text{m}^2/\text{s}$ and cell volume $V \simeq 3{,}000\,\mu\text{m}^3$. In this case the buffering strength differs from noise reduction by more than 2-fold (Figure 2B, red and blue dots and inset, red dot). Note that applying our theory to *in vivo* situations, D is an effective diffusion constant that may depend on more complex molecular kinetics than simple diffusion. In summary, concentration buffering and noise reduction are distinct concepts, which become similar only in the extreme case of a very large and slowly varying system.

Multicomponent systems can effectively buffer concentration and reduce noise

To generalize our analysis, we consider a three-component system, with both solutes A and B being present. For simplicity, we focus on the extreme case of a purely heterotypic system, where $\chi_{AS} = \chi_{BS} = 0$ and $\chi_{AB} < 0$. The stochastic processes r_A and r_B are considered to be independent but identical birth-and-death processes with mean $\langle r\rangle = \lambda_1/\lambda_2$ and autocovariance function $\kappa(\tau) = \lambda_1/\lambda_2 e^{-\lambda_2\tau}$ as before. In the following, we focus on noise reduction and concentration buffering of solute A, but equivalent analyses apply to the second solute B. In line with previous observations,[2,5,7] this system displays a more complex concentration dependence, such that even at equilibrium, the average dilute phase concentration changes substantially with average total concentration (Figure 2C, black line). The concentration dependence is further affected by the presence of synthesis and turnover of solutes A and B (Figure 2C, blue line). As in the binary case, the buffering strength varies across different $\langle\phi\rangle$ but in our example takes large values overall. Also, noise is reduced for a broad range of $\langle\phi\rangle$, even though $\langle\phi_1\rangle$ varies substantially. These results are in line with experimental measurements of nucleolar component nucleophosmin (NPM1),[7,11] where dilute phase NPM1 concentration increased substantially upon overexpression,[7] while endogenous labeling of NPM1 revealed that noise reduction occurred at the physiological setpoint[11] (Figure S2B).

We further considered the case, where fluctuations in components A and B are positively correlated (Figure 2D). This is inspired by previous theoretical work showing that coexisting concentrations of macroscopic systems are buffered when the total concentrations $\langle\phi\rangle$ and $\langle\psi\rangle$ vary quasi-statically along tie lines.[2] Tie lines connect the coexisting compositions in a phase diagram. When variations of total concentrations occur along a tie line, the coexisting compositions at equilibrium do not change, while they do change if variations are not along a tie line.[2,5] Our analysis extends this concept to mesoscopic non-equilibrium systems where ϕ and ψ fluctuate on finite timescales. To account for correlations between ϕ and ψ, we consider the case where the same birth-process drives the synthesis of both components A and B, i.e.,

Please cite this article in press as: Zechner and Jülicher, Concentration buffering and noise reduction in non-equilibrium phase-separating systems, Cell Systems (2025), https://doi.org/10.1016/j.cels.2025.101168

$r_A = r_B = r$ with mean and autocovariance function as defined above. This leads to a positive correlation between ϕ and ψ, which can be aligned with a tie line. While the predicted average concentrations $\langle\phi\rangle$ and $\langle\phi_1\rangle$ are not affected by the presence of correlations between ϕ and ψ (compare blue lines in Figures 2C and 2D), we find fluctuations of dilute phase concentration to depend in a notable manner on such correlations. In our example, fluctuations in total concentration ϕ and dilute phase concentration ϕ_1 are positively correlated for small $\langle\phi\rangle$, similarly to the case where ϕ and ψ are uncorrelated (Figure 2D). For larger $\langle\phi\rangle$, however, the correlations between ϕ and ϕ_1 become negative, meaning that at the level of individual realizations (e.g., cells in a population), fluctuations leading to larger ϕ are associated with smaller ϕ_1. At the same time, the average concentrations show the opposite behavior and $\langle\phi_1\rangle$ increases with increasing $\langle\phi\rangle$ (Figure 2D). This difference in behavior arises because in the case of average concentrations, buffering is characterized by the response of $\langle\phi_1\rangle$ to changes in $\langle\phi\rangle$, while noise in ϕ_1 is governed by correlated fluctuations of several variables. The exact statistics of ϕ_1 depend on the interplay between the thermodynamic and kinetic features of the system. This demonstrates that buffering of averages and the behavior of fluctuations around averages can show very different behaviors. Moreover, while the buffering strength was consistently larger than noise reduction in our previous examples (Figures 2B and 2C, inset), this is no longer true when fluctuations in ϕ and ψ are correlated. In this example, noise reduction can be smaller or larger than the buffering strength, depending on the set-point $\langle\phi\rangle$ (Figure 2D, inset). This analysis further illustrates that concentration buffering and noise reduction provide different insights into phase-separating systems and that in general, one cannot be inferred from the other.

A fixed saturation concentration implies effective concentration buffering but not noise reduction

So far, we have demonstrated that a fixed saturation concentration is not necessary for noise reduction and concentration buffering to occur. We next analyzed whether a fixed saturation concentration guarantees noise reduction and concentration buffering. To do so, we considered an example of a two-component system with fast phase-separation dynamics exhibiting a weak dilute phase dependence g_{NE} on total concentration, resulting in a large buffering strength (Figures S3A and S3B, blue lines). Moreover, the parameters were chosen such that noise in total concentration was smaller than in the examples discussed above where noise reduction had been significant. In this case, even though partitioning is very fast on the timescale of solute turnover, noise reduction fails (Figures S3A inset and S3B red line). This is because noise reduction relies on partitioning noise to be weaker than the non-equilibrium fluctuations arising from protein production and degradation. As we have shown previously, partitioning noise therefore forms a lower bound on noise in the considered phase-separating systems.[11] In summary, while a fixed saturation concentration ensures effective concentration buffering, it is not sufficient for noise reduction to take place.

Conclusions

Using a series of examples, we have clarified the relationship between concentration buffering and noise reduction by phase-separated compartments. We show that these two concepts are different and become similar only for large systems near thermodynamic equilibrium, i.e., if the composition varies slowly. In this special case, noise reduction can be related to concentration buffering governed by equilibrium phase diagrams.[2,13] As we have shown, however, these concepts can be substantially different when non-equilibrium fluctuations have a finite correlation time and when the finite system size is taken into account. In general, concentration buffering can neither predict noise reduction nor can it provide bounds on it.

Inspired by previous discussions,[7,12,13] we have tested to what extent a fixed saturation concentration is important for noise reduction. We have shown that two-component and multicomponent systems lacking fixed saturation concentrations can nevertheless reduce noise effectively. Conversely, we have shown that systems exhibiting a fixed saturation concentration may fail to suppress noise or may even increase it. Thus, a fixed saturation concentration is neither necessary nor sufficient for effective noise reduction to take place. If and to what extent a phase-separated compartment reduces noise depends on the interplay between the thermodynamic and kinetic properties of that compartment.

Our results have broader implications for the analysis of intracellular condensates. As an example, it has been suggested that when the titration of a component leads to a change in dilute phase concentration, or the partition coefficient, this points toward heterotypic interactions governing the formation of these condensates.[5,7,24] This argument is based on equilibrium phase diagrams of multicomponent mixtures. However, our analysis shows that in the presence of non-equilibrium production and turnover, variable dilute phase concentrations and variable partition coefficients arise generically, independent of the type of the underlying interactions. Since in cells, material is subject to production and turnover, inference of interactions based on equilibrium phase diagrams is thus unreliable.

An important challenge in the condensate field is to understand how far traditional concepts from condensed matter physics can take us in studying intracellular compartments and where new concepts may be needed. Moving from simpler systems comprising few components to systems with larger compositional complexity is an important goal in this regard.[2,7,24] At the same time, we have to account for the dynamic complexity of cellular systems arising from stochastic, non-equilibrium processes.[11,14,22,25] Developing theoretical and experimental approaches to study noise and information processing in non-equilibrium multicomponent condensates will remain an important challenge in the future.

RESOURCE AVAILABILITY

Lead contact

Further information and requests for resources should be directed to and will be fulfilled by the lead contact, Christoph Zechner (czechner@sissa.it).

Materials availability

This study did not generate new materials.

Data and code availability

- This paper analyzes existing, publicly available data. Access information is provided in the key resources table.
- All original code has been deposited at Zenodo and is publicly available as of the date of publication. DOIs are listed in the key resources table.

- Any additional information required to reanalyze the data reported in this paper is available from the lead contact upon request.

ACKNOWLEDGMENTS

We are grateful to Titus Franzmann, Tyler Harmon, Alf Honigmann, Anthony Hyman, Adam Klosin, Andrea Musacchio, Florian Oltsch, Akshaye Pal, and David Zwicker for stimulating discussions and feedback. The authors thank the MPI-CBG, the MPI-PKS, and the Max Planck Society for supporting this work. C.Z. acknowledges funding from the Deutsche Forschungsgemeinschaft (DFG, German Research Foundation) (ZE1216/1-1).

AUTHOR CONTRIBUTIONS

C.Z. and F.J. did this work together and wrote the paper together.

DECLARATION OF INTERESTS

The authors declare no competing interests.

STAR★METHODS

Detailed methods are provided in the online version of this paper and include the following:

- KEY RESOURCES TABLE
- METHOD DETAILS
  - Equilibrium theory
  - Kinetics of solute and solvent partitioning
  - Accounting for non-equilibrium production and turnover of solutes
  - Droplet kinetics in the presence of non-equilibrium production and turnover of solutes
  - Analytical results for the case of a two-component mixture
  - Noise reduction in the limit of large volumes and quasi-static birth-rates
- QUANTIFICATION AND STATISTICAL ANALYSIS
  - Synthetic system
  - Endogenous system

SUPPLEMENTAL INFORMATION

Supplemental information can be found online at https://doi.org/10.1016/j.cels.2025.101168.

Received: April 12, 2024
Revised: October 10, 2024
Accepted: January 2, 2025
Published: February 7, 2025

REFERENCES

1. Banani, S.F., Lee, H.O., Hyman, A.A., and Rosen, M.K. (2017). Biomolecular condensates: organizers of cellular biochemistry. Nat. Rev. Mol. Cell Biol. *18*, 285–298.
2. Deviri, D., and Safran, S.A. (2021). Physical theory of biological noise buffering by multicomponent phase separation. Proc. Natl. Acad. Sci. USA *118*, e2100099118.
3. Jacobs, W.M., and Frenkel, D. (2017). Phase transitions in biological systems with many components. Biophys. J. *112*, 683–691.
4. Jacobs, W.M., and Frenkel, D. (2013). Predicting phase behavior in multicomponent mixtures. J. Chem. Phys. *139*, 024108.
5. Choi, J.M., Dar, F., and Pappu, R.V. (2019). Lassi: A lattice model for simulating phase transitions of multivalent proteins. PLoS Comput. Biol. *15*, e1007028.
6. Mao, S., Kuldinow, D., Haataja, M.P., and Košmrlj, A. (2019). Phase behavior and morphology of multicomponent liquid mixtures. Soft Matter *15*, 1297–1311.
7. Riback, J.A., Zhu, L., Ferrolino, M.C., Tolbert, M., Mitrea, D.M., Sanders, D.W., Wei, M.T., Kriwacki, R.W., and Brangwynne, C.P. (2020). Composition-dependent thermodynamics of intracellular phase separation. Nature *581*, 209–214.
8. Graf, I.R., and Machta, B.B. (2022). Thermodynamic stability and critical points in multicomponent mixtures with structured interactions. Phys. Rev. Res. *4*, 033144.
9. Holehouse, A.S., and Pappu, R.V. (2018). Functional implications of intracellular phase transitions. Biochemistry *57*, 2415–2423.
10. Stoeger, T., Battich, N., and Pelkmans, L. (2016). Passive noise filtering by cellular compartmentalization. Cell *164*, 1151–1161.
11. Klosin, A., Oltsch, F., Harmon, T., Honigmann, A., Jülicher, F., Hyman, A.A., and Zechner, C. (2020). Phase separation provides a mechanism to reduce noise in cells. Science *367*, 464–468.
12. Chattaraj, A., Blinov, M.L., and Loew, L.M. (2021). The solubility product extends the buffering concept to heterotypic biomolecular condensates. eLife *10*, e67176.
13. Riback, J.A., and Brangwynne, C.P. (2020). Can phase separation buffer cellular noise? Science *367*, 364–365.
14. Rosenfeld, N., Young, J.W., Alon, U., Swain, P.S., and Elowitz, M.B. (2005). Gene regulation at the single-cell level. Science *307*, 1962–1965.
15. Suter, D.M., Molina, N., Gatfield, D., Schneider, K., Schibler, U., and Naef, F. (2011). Mammalian genes are transcribed with widely different bursting kinetics. Science *332*, 472–474.
16. Larson, D.R., Zenklusen, D., Wu, B., Chao, J.A., and Singer, R.H. (2011). Real-time observation of transcription initiation and elongation on an endogenous yeast gene. Science *332*, 475–478.
17. Lestas, I., Vinnicombe, G., and Paulsson, J. (2010). Fundamental limits on the suppression of molecular fluctuations. Nature *467*, 174–178.
18. Sartori, P., and Tu, Y. (2015). Free energy cost of reducing noise while maintaining a high sensitivity. Phys. Rev. Lett. *115*, 118102.
19. De Gennes, P.G. (1979). Scaling Concepts in Polymer Physics (Cornell University Press).
20. Flory, P.J. (1953). Principles of Polymer Chemistry (Cornell University Press).
21. Paulsson, J. (2004). Summing up the noise in gene networks. Nature *427*, 415–418.
22. Elowitz, M.B., Levine, A.J., Siggia, E.D., and Swain, P.S. (2002). Stochastic gene expression in a single cell. Science *297*, 1183–1186.
23. van Kampen, N.D. (1992). Stochastic processes in physics and chemistry (Elsevier).
24. Mittag, T., and Pappu, R.V. (2022). A conceptual framework for understanding phase separation and addressing open questions and challenges. Mol. Cell *82*, 2201–2214.
25. Battle, C., Broedersz, C.P., Fakhri, N., Geyer, V.F., Howard, J., Schmidt, C.F., and MacKintosh, F.C. (2016). Broken detailed balance at mesoscopic scales in active biological systems. Science *352*, 604–607.
26. Yan, V.T., Narayanan, A., Wiegand, T., Jülicher, F., and Grill, S.W. (2022). A condensate dynamic instability orchestrates actomyosin cortex activation. Nature *609*, 597–604.
27. Taniguchi, Y., Choi, P.J., Li, G.W., Chen, H.Y., Babu, M., Hearn, J., Emili, A., and Xie, X.S. (2010). Quantifying E-coli proteome and transcriptome with single-molecule sensitivity in single cells. Science *329*, 533–538.
28. Schwanhäusser, B., Busse, D., Li, N., Dittmar, G., Schuchhardt, J., Wolf, J., Chen, W., and Selbach, M. (2011). Global quantification of mammalian gene expression control. Nature *473*, 337–342.
29. Eden, E., Geva-Zatorsky, N., Issaeva, I., Cohen, A., Dekel, E., Danon, T., Cohen, L., Mayo, A., and Alon, U. (2011). Proteome half-life dynamics in living human cells. Science *331*, 764–768.

30. Shin, Y., Berry, J., Pannucci, N., Haataja, M.P., Toettcher, J.E., and Brangwynne, C.P. (2017). Spatiotemporal control of intracellular phase transitions using light-activated optodroplets. Cell *168*, 159–171.e14.

31. Wheeler, J.R., Matheny, T., Jain, S., Abrisch, R., and Parker, R. (2016). Distinct stages in stress granule assembly and disassembly. eLife *5*, e18413.

32. Bar-Even, A., Paulsson, J., Maheshri, N., Carmi, M., O'Shea, E., Pilpel, Y., and Barkai, N. (2006). Noise in protein expression scales with natural protein abundance. Nat. Genet. *38*, 636–643.

33. Munsky, B., Neuert, G., and Van Oudenaarden, A. (2012). Using gene expression noise to understand gene regulation. Science *336*, 183–187.

34. Schiff, J.L. (2013). The Laplace Transform: Theory and Applications (Springer Science & Business Media).

35. Brangwynne, C.P., Eckmann, C.R., Courson, D.S., Rybarska, A., Hoege, C., Gharakhani, J., Jülicher, F., and Hyman, A.A. (2009). Germline p granules are liquid droplets that localize by controlled dissolution/condensation. Science *324*, 1729–1732.

36. Efron, B. (1979). Bootstrap methods: another look at the jackknife. Ann. Statist. *7*, 1–26.

37. Robert, C.P., and Casella, G. (1999). Monte Carlo Statistical Methods*2* (Springer).

38. Freibaum, B.D., Messing, J., Yang, P., Kim, H.J., and Taylor, J.P. (2021). High-fidelity reconstitution of stress granules and nucleoli in mammalian cellular lysate. J. Cell Biol. *220*, e202009079.

Please cite this article in press as: Zechner and Jülicher, Concentration buffering and noise reduction in non-equilibrium phase-separating systems, Cell Systems (2025), https://doi.org/10.1016/j.cels.2025.101168

STAR★METHODS

KEY RESOURCES TABLE

REAGENT or RESOURCE	SOURCE	IDENTIFIER
Software and algorithms		
MATLAB source code	This paper	https://doi.org/10.5281/zenodo.14413285
2NT-DDX4^{YFP} data	Klosin et al.[11]	N/A
NPM1-NeonGreen data	Klosin et al.[11]	N/A
NPM1-mCherry data	Riback et al.[7]	N/A
MATLAB	The MathWorks Inc., Natick, Massachusetts	version 9.10.0.1602886 (R2021a)

METHOD DETAILS

Equilibrium theory

We consider a system comprising two solutes A and B and solvent S, which phase-separates into two phases of volumes V_1 and V_2, where V_2 is a droplet. The free energy of this system is written as

$$F = V_1 f(\phi_1, \psi_1) + V_2 f(\phi_2, \psi_2) + \gamma \mathcal{A}_2, \quad \text{(Equation 10)}$$

with $\mathcal{A}_2 = (36\pi)^{1/3} V_2^{2/3}$ as the surface area of the droplet and γ denoting surface tension. For the free energy density f of a homogeneous phase, we consider a ternary Flory-Huggins model

$$f(\phi,\psi) = \frac{k_B T}{v}\Big[\chi_{AS}\phi(1-\phi-\psi) + \chi_{AB}\phi\psi + \chi_{BS}\psi(1-\phi-\psi) + \frac{\phi}{n}\log\phi + \frac{\psi}{n}\log\psi + (1-\phi-\psi)\log(1-\phi-\psi)\Big], \quad \text{(Equation 11)}$$

with effective interaction parameters χ_{AS}, χ_{AB} and χ_{BS}. For simplicity, we consider the case where the solutes A and B have identical molecular volume nv with v denoting the molecular volume of solvent S and n as a positive number. We choose to describe the system using the degrees of freedom a_1, b_1 and s_1, corresponding to the copy numbers of A, B and S molecules in the dilute phase of volume V_1, respectively. We then have $\phi_1 = a_1 nv/V_1$, $\psi_1 = b_1 nv/V_1$, $V_1 = v(a_1 n + b_1 n + s_1)$ and we use $a_1 = a - a_1$, $b_2 = b - b_1$ and $V_2 = V - V_1$ due to particle number conservation ($a = a_1 + a_2$ and $b = b_1 + b_2$) and incompressibility ($V = V_1 + V_2 = const.$). In terms of the degrees of freedom a_1, b_1 and s_1, the free energy reads

$$F(a_1,b_1,s_1) = v(a_1 n + b_1 n + s_1) f\left(\frac{a_1 n}{a_1 n + b_1 n + s_1}, \frac{b_1 n}{a_1 n + b_1 n + s_1}\right) + [V - v(a_1 n + b_1 n + s_1)] f\left(\frac{(a-a_1)nv}{V - v(a_1 n + b_1 n + s_1)}, \frac{(b-b_1)nv}{V - v(a_1 n + b_1 n + s_1)}\right) + \gamma(36\pi)^{1/3}[V - v(a_1 n + b_1 n + s_1)]^{2/3}. \quad \text{(Equation 12)}$$

At equilibrium, a_1, b_1 and s_1 exhibit Boltzmann statistics

$$P_{EQ}(a_1,b_1,s_1|a,b) = \frac{1}{Z} e^{-\frac{F(a_1,b_1,s_1)}{k_B T}}, \quad \text{(Equation 13)}$$

where

$$Z = \sum_{(a_1,b_1,s_1)\in\mathcal{S}} e^{-\frac{F(a_1,b_1,s_1)}{k_B T}} \quad \text{(Equation 14)}$$

is the partition function and $\mathcal{S} = [0,a] \times [0,b] \times [0, V/v - n(a+b)]$. Equilibrium quantities can be determined by calculating moments of the Boltzmann distribution as a function of a or b. In case of solute A, for instance, we define

$$\langle \phi_1 | \phi, \psi \rangle = \langle \phi_1 | a, b \rangle = \sum_{(a_1,b_1,s_1)\in\mathcal{S}} \frac{a_1 n}{a_1 n + b_1 n + s_1} P_{EQ}(a_1,b_1,s_1|a,b). \quad \text{(Equation 15)}$$

In Equation 15, the symbol $\langle \phi_1 | \phi, \psi \rangle$ denotes the conditional expectation of ϕ_1 given a particular ϕ and ψ. As we are interested in how the dilute phase concentration of one component (e.g., ϕ_1) changes with total concentration of the same component (e.g., ϕ) we

Please cite this article in press as: Zechner and Jülicher, Concentration buffering and noise reduction in non-equilibrium phase-separating systems, Cell Systems (2025), https://doi.org/10.1016/j.cels.2025.101168

CellPress
OPEN ACCESS

will drop the dependency on total concentration of the other component (e.g., ψ) in our notation. In case of component A, for instance, we define

$$g(\phi) = \langle \phi_1 | \phi, \psi \rangle \quad \text{(Equation 16)}$$

as ψ is fixed. For sufficiently abundant systems with approximately Gaussian fluctuations, the above expectation may be approximated by the minimum of the free energy, or equivalently, the mode of the underlying Boltzmann distribution and we will use this approximation when calculating equilibrium concentration dependencies. Numerically, the minimum of the free energy was determined using the *fmincon* function of MATLAB (version 9.10.0.1602886 (R2021a), The MathWorks Inc., Natick, Massachusetts), using the interior-point algorithm under default settings.

Kinetics of solute and solvent partitioning

To study concentration fluctuations in non-equilibrium conditions (see STAR Methods section "Accounting for non-equilibrium production and turnover of solutes"), we require a kinetic description of the considered phase-separating system. To this end, we consider three pairs of molecular exchange events

$$(a_1, b_1, s_1) \underset{w_A^+}{\overset{w_A^-}{\rightleftarrows}} (a_1 - 1, b_1, s_1 + n) \quad \text{(Equation 17)}$$

$$(a_1, b_1, s_1) \underset{w_B^+}{\overset{w_B^-}{\rightleftarrows}} (a_1, b_1 - 1, s_1 + n) \quad \text{(Equation 18)}$$

$$(a_1, b_1, s_1) \underset{w_S^+}{\overset{w_S^-}{\rightleftarrows}} (a_1, b_1, s_1 - 1). \quad \text{(Equation 19)}$$

The first two rows correspond to exchange of solutes A and B in and out of the dense phase, while the third row captures volume fluctuations of the phases due to solvent exchange. These events are driven by generalized thermodynamic forces. Thermodynamics requires the rates to obey the following conditions

$$\log \frac{w_A^-(a_1, b_1, s_1)}{w_A^+(a_1 - 1, b_1, s_1 + n)} = -\frac{1}{k_B T}\left[F(a_1 - 1, b_1, s_1 + n) - F(a_1, b_1, s_1)\right] \quad \text{(Equation 20)}$$

$$\log \frac{w_B^-(a_1, b_1, s_1)}{w_B^+(a_1, b_1 - 1, s_1 + n)} = -\frac{1}{k_B T}\left[F(a_1, b_1 - 1, s_1 + n) - F(a_1, b_1, s_1)\right] \quad \text{(Equation 21)}$$

$$\log \frac{w_S^-(a_1, b_1, s_1)}{w_S^+(a_1, b_1, s_1 - 1)} = -\frac{1}{k_B T}\left[F(a_1, b_1, s_1 - 1) - F(a_1, b_1, s_1)\right], \quad \text{(Equation 22)}$$

where $w_A^{+/-}$, $w_B^{+/-}$ and $w_S^{+/-}$ are event probabilities per unit time. Considering copy numbers to be sufficiently large, the free energy differences in Equations 20, 21, and 22 can be approximated as directional derivatives. More precisely, we approximate $F(a_1 + \nu_a, b_1 + \nu_b, s_1 + \nu_s) - F(a_1, b_1, s_1) \simeq (\nu_a\ \nu_b\ \nu_s)\nabla F(a_1, b_1, s_1)$, with $\nabla F(a_1, b_1, s_1) = (\partial_{a_1}\ \partial_{b_1}\ \partial_{s_1})^T F(a_1, b_1, s_1)$ as the gradient of the free energy. This leads to

$$\log \frac{w_A^-(a_1, b_1, s_1)}{w_A^+(a_1 - 1, b_1, s_1 + n)} = -\begin{pmatrix} -1 & 0 & n \end{pmatrix}\nabla F(a_1, b_1, s_1) = -\frac{n v}{k_B T}\left(\mu_2^A - \mu_1^A\right) \quad \text{(Equation 23)}$$

$$\log \frac{w_B^-(a_1, b_1, s_1)}{w_B^+(a_1, b_1 - 1, s_1 + n)} = -\begin{pmatrix} 0 & -1 & n \end{pmatrix}\nabla F(a_1, b_1, s_1) = -\frac{n v}{k_B T}\left(\mu_2^B - \mu_1^B\right) \quad \text{(Equation 24)}$$

$$\log \frac{w_S^-(a_1, b_1, s_1)}{w_S^+(a_1, b_1, s_1 - 1)} = -\begin{pmatrix} 0 & 0 & -1 \end{pmatrix}\nabla F(a_1, b_1, s_1) = -\frac{v}{k_B T}\left[\Pi_2 - \Pi_1\right] - \frac{\gamma}{k_B T}\partial_{s_1}\mathcal{A}_2, \quad \text{(Equation 25)}$$

where $\mu_\alpha^A = \partial_{\phi_\alpha} f(\phi_\alpha, \psi_\alpha)$ and $\mu_\alpha^B = \partial_{\psi_\alpha} f(\phi_\alpha, \psi_\alpha)$ are the exchange chemical potential of component A and B in phase $\alpha \in \{1,2\}$, $\Pi_2 - \Pi_1$ is the osmotic pressure difference with $\Pi_\alpha = f(\phi_\alpha, \psi_\alpha) - \phi\mu_\alpha^A - \psi\mu_\alpha^B$ and $\gamma\partial_{s_1}\mathcal{A}_2/v$ is the Laplace pressure.

Please cite this article in press as: Zechner and Jülicher, Concentration buffering and noise reduction in non-equilibrium phase-separating systems, Cell Systems (2025), https://doi.org/10.1016/j.cels.2025.101168

We choose the partitioning of solutes into the dense phase to be diffusion-limited with $w_A^+(a_1,b_1,s_1) = 6D/V_1^{2/3}a_1$ and $w_B^+(a_1,b_1,s_1) = 6D/V_1^{2/3}b_1$, where we consider the two solutes A and B to have the same diffusion constant D for simplicity. The corresponding reverse rates w_A^- and w_B^- are then chosen to satisfy (Equation 23) and (Equation 24). Solvent exchange (Equation 19) is expected to be fast on the timescale of solute exchange, effectively keeping the system close to osmotic equilibrium. We therefore consider the limit where the kinetic coefficients associated with w_S^+ and w_S^- are fast in comparison to solute exchange, effectively eliminating one kinetic mode of this system. Practically, this was achieved by choosing $w_S^-(a_1,b_1,s_1) = k_S$, determining the reverse rate w_s^+ to satisfy Equation 25 and setting the kinetic coefficient k_S to large values (see Tables S1–S5).

Accounting for non-equilibrium production and turnover of solutes

In the presence of noise, the total concentrations ϕ and ψ are no longer conserved. To describe solute fluctuations, we use stochastic birth-and-death processes with fluctuating birth-rates.[21,27,32,33] We describe synthesis and turnover of a component $X \in \{A,B\}$ as

$$(x,s) \underset{w_X^d}{\overset{w_X^b}{\rightleftarrows}} (x+1, s-n), \tag{Equation 26}$$

where whenever a molecule X is produced or degraded, n solvent molecules are removed or added to the system, leaving the total volume conserved. We further set $w_X^b = Vk_1^X r_X(t)$ where k_1^X is a birth-rate per volume and $w_X^d = k_2 x(t)$ with $x(t)$ as the copy number of molecule X. For simplicity we consider the case where both solutes A and B are degraded with the same rate constant k_2. The stochastic process $r_X(t)$ captures fluctuations in the synthesis rate, for instance due to transcriptional noise or extrinsic variability. We consider $r_X(t)$ to be a stationary stochastic process with mean $\langle r_X\rangle$ and autocovariance function $\kappa_X(\tau) = \langle r_X(t) r_X(t+\tau)\rangle - \langle r_X\rangle^2$ for $X \in \{A,B\}$. In the presence of phase coexistence, both synthesis and turnover events can take place in both phases $i = \{1,2\}$ with rates $w_{X,i}^b = V_i k_1^X r_X(t)$ and $w_{X,i}^d = k_2 x_i(t)$, leaving the statistics of total concentration ϕ and ψ unchanged. This choice is useful to compare fluctuations in the presence and absence of phase coexistence. Note that in order to avoid negative solvent copy numbers, we require $w_{X,i}^b = 0$ if $s_i < n$. However, since we consider regimes where solvent molecules are much more abundant than solute molecules, we neglect this constraint in our calculations. In the following, we will denote by $\mathcal{BD}(w_X^b, w_X^d)$ a birth-and-death process X with birth-rate w_X^b and death-rate w_X^d.

To derive the statistics of total solute concentration, we consider the birth-and-death process $\mathcal{BD}(Vk_1 r(t), k_2 x(t))$. For a particular realization of the process $r(t)$, the probability of having x molecules at time t can be described by a master equation

$$\begin{aligned}\frac{d}{dt}P(x,t) = {} & Vk_1 r(t) P(x-1,t) + k_2(x+1)P(x+1,t) \\ & - [Vk_1 r(t) + k_2 x] P(x,t),\end{aligned} \tag{Equation 27}$$

with $P(x,t) := P(x(t)|r_0^t)$ as the copy number distribution of molecules X at time t given a realization r_0^t of the process $r(t)$. The conditional mean and variance of x can be obtained from Equation 27 and are given by

$$\langle x(t)|r_0^t\rangle = \mathrm{Var}\left[x(t)|r_0^t\right] = Vk_1 \int_0^t e^{-k_2(t-\tau)} r(\tau) d\tau, \tag{Equation 28}$$

where we have chosen $\langle x(0)|r_0\rangle = \mathrm{Var}[x(0)|r_0] = 0$ for convenience (the initial conditions are irrelevant since we are interested in the long term behavior). The stationary mean of $x(t)$ is readily obtained by taking the expectation of Equation 28 and letting $t \to \infty$, which yields

$$\langle x\rangle = \frac{Vk_1\langle r\rangle}{k_2}. \tag{Equation 29}$$

For the variance of $x(t)$, we make use of the law of total variance, which states that

$$\mathrm{Var}[x(t)] = \langle \mathrm{Var}\left[x(t)|r_0^t\right]\rangle + \mathrm{Var}\left[\langle x(t)|r_0^t\rangle\right]. \tag{Equation 30}$$

The first term on the rhs of Equation 30 is the same as the stationary mean, i.e., $\langle \mathrm{Var}[x(t)|r_0^t]\rangle \xrightarrow{t\to\infty} k_1 V\langle r\rangle/k_2$. The second term on the rhs of Equation 30 is given by

$$\begin{aligned}\mathrm{Var}\left[\langle x(t)|r_0^t\rangle\right] &= \mathrm{Var}\left[Vk_1 \int_0^t e^{-k_2(t-\tau)} r(\tau) d\tau\right] \\ &= (k_1 V)^2 e^{-2k_2 t} \mathrm{Var}\left[\int_0^t e^{k_2\tau} r(\tau) d\tau\right].\end{aligned} \tag{Equation 31}$$

The variance of the integral can be rewritten as

Please cite this article in press as: Zechner and Jülicher, Concentration buffering and noise reduction in non-equilibrium phase-separating systems, Cell Systems (2025), https://doi.org/10.1016/j.cels.2025.101168

CellPress
OPEN ACCESS

$$\begin{aligned}\mathrm{Var}\left[\int_0^t e^{k_2\tau} r(\tau)d\tau\right] &= \left\langle\left(\int_0^t e^{k_2\tau} r(\tau)d\tau\right)^2\right\rangle - \left(\int_0^t e^{k_2\tau}\langle r(\tau)\rangle d\tau\right)^2 \\ &= \int_0^t\int_0^t e^{k_2(\tau+\tau')}\langle r(\tau)r(\tau')\rangle d\tau d\tau' - \int_0^t\int_0^t e^{k_2(\tau+\tau')}\langle r(\tau)\rangle\langle r(\tau')\rangle d\tau d\tau' \\ &= \int_0^t\int_0^t e^{k_2(\tau+\tau')}\kappa(\tau'-\tau)d\tau d\tau'.\end{aligned} \quad \text{(Equation 32)}$$

Using the fact that the autcovariance $\kappa(\tau) = \langle r(t)\, r(t+\tau)\rangle - \langle r\rangle^2$ is time-symmetric, we can simplify this expression to

$$\begin{aligned}&\int_0^t\int_0^t e^{k_2(\tau+\tau')}\kappa(\tau'-\tau)d\tau d\tau' \\ &= \int_0^t\int_{\tau'}^t e^{k_2(\tau+\tau')}\kappa(\tau'-\tau)d\tau d\tau' + \int_0^t\int_0^{\tau'} e^{k_2(\tau+\tau')}\kappa(\tau'-\tau)d\tau d\tau' \\ &= \int_0^t\int_0^{\tau} e^{k_2(\tau+\tau')}\kappa(\tau-\tau')d\tau' d\tau + \int_0^t\int_0^{\tau'} e^{k_2(\tau+\tau')}\kappa(\tau'-\tau)d\tau d\tau' \\ &= 2\int_0^t\int_0^{\tau'} e^{k_2(\tau+\tau')}\kappa(\tau'-\tau)d\tau d\tau'\end{aligned} \quad \text{(Equation 33)}$$

The variance of the conditional mean is thus given by

$$\mathrm{Var}\left[\langle x(t)|r_0^t\rangle\right] = 2(k_1V)^2 e^{-2k_2t}\int_0^t\int_0^{\tau'} e^{k_2(\tau+\tau')}\kappa(\tau'-\tau)d\tau d\tau'. \quad \text{(Equation 34)}$$

We next calculate the Laplace transform of this equation, which will allow us to determine a general expression for $\mathrm{Var}[\langle x(t)|r_0^t\rangle]$ in the limit of $t\to\infty$. To this end, we first rewrite Equation 34 as

$$\mathrm{Var}\left[\langle x(t)|r_0^t\rangle\right] = 2(k_1V)^2 e^{-2k_2t}\int_0^t e^{k_2\tau'}\int_0^{\tau'} e^{k_2\tau}\kappa(\tau'-\tau)d\tau d\tau', \quad \text{(Equation 35)}$$

such that the inner integral now has the form of a convolution integral. To calculate the Laplace transform of Equation 35, we make use of the properties[34]

$$\mathcal{L}\left\{\int_0^t g(s)f(t-s)ds\right\} = \widehat{g}(u)\widehat{f}(u) \quad \text{(Equation 36)}$$

$$\mathcal{L}\{e^{\beta t}g(t)\} = \widehat{g}(u-\beta) \quad \text{(Equation 37)}$$

$$\mathcal{L}\left\{\int_0^t g(s)ds\right\} = \frac{1}{u}\widehat{g}(u), \quad \text{(Equation 38)}$$

where $\widehat{g}(u) = \int_0^\infty g(t)e^{-ut}dt$ and $\widehat{f}(u) = \int_0^\infty f(t)e^{-ut}dt$ are the one-sided Laplace transforms of functions g and f, respectively and β is a constant. Using these properties, we obtain

$$\mathcal{L}\left\{\mathrm{Var}\left[\langle x(t)|r_0^t\rangle\right]\right\} = \frac{2(k_1V)^2}{u(u+2k_2)}\widehat{\kappa}(u+k_2), \quad \text{(Equation 39)}$$

with $\widehat{\kappa}(u) = \int_0^\infty \kappa(t)e^{-ut}dt$ as the Laplace transform of the autocovariance function κ. Further using the property $\lim_{t\to\infty} g(t) = \lim_{u\to 0} u\widehat{g}(u)$,[34] we obtain for the long-term variance of the conditional mean (assuming that it exists)

$$\lim_{t\to\infty}\mathrm{Var}\left[\langle x(t)|r_0^t\rangle\right] = \lim_{u\to 0}\frac{2(k_1V)^2}{u+2k_2}\widehat{\kappa}(u+k_2) = \frac{(k_1V)^2}{k_2}\widehat{\kappa}(k_2). \quad \text{(Equation 40)}$$

Please cite this article in press as: Zechner and Jülicher, Concentration buffering and noise reduction in non-equilibrium phase-separating systems, Cell Systems (2025), https://doi.org/10.1016/j.cels.2025.101168

In total, we obtain for the stationary variance of $x(t)$

$$\mathrm{Var}[x] = V\frac{k_1}{k_2}\langle r\rangle + \frac{(k_1V)^2}{k_2}\widehat{\kappa}(k_2). \quad \text{(Equation 41)}$$

The relative noise defined as the squared coefficient of variation $\eta^2[x] = \mathrm{Var}[x]/\langle x\rangle^2$ is given by

$$\eta^2[x] = \frac{1}{V}\frac{k_2}{k_1\langle r\rangle} + \frac{k_2}{\langle r\rangle^2}\widehat{\kappa}(k_2). \quad \text{(Equation 42)}$$

The first term on the right-hand side of Equation 42 can be identified as $1/\langle x\rangle$ and thus exhibits Poissonian scaling. The second term quantifies the amount of noise that propagates from $r(t)$ to x, which depends on the timescales of $r(t)$ through the autocovariance function κ.

Note that the noise strength $\eta^2[x]$ is invariant upon rescaling of x such that Equation 42 applies also to the concentration (and volume fraction) of X. The noise strength of total concentrations ϕ and ψ can be obtained by applying Equation 42 to the birth-and-death processes $\mathcal{BD}(Vk_1^A r_A(t), k_2 a(t))$ and $\mathcal{BD}(Vk_1^B r_B(t), k_2 b(t))$, i.e.,

$$\eta^2[\phi] = \frac{1}{V}\frac{k_2}{k_1^A\langle r_A\rangle} + \frac{k_2}{\langle r_A\rangle^2}\widehat{\kappa}_A(k_2) \quad \text{(Equation 43)}$$

$$\text{and} \quad \eta^2[\psi] = \frac{1}{V}\frac{k_2}{k_1^B\langle r_B\rangle} + \frac{k_2}{\langle r_B\rangle^2}\widehat{\kappa}_B(k_2). \quad \text{(Equation 44)}$$

Droplet kinetics in the presence of non-equilibrium production and turnover of solutes

To study how non-equilibrium fluctuations in total concentration are affected by phase coexistence, we consider a system that accounts for solute and solvent partitioning as well as synthesis and degradation of molecules in each phase. The state of this system is characterized by seven degrees of freedom $(a_1(t), b_1(t), s_1(t), a(t), b(t), r_A(t), r_B(t))$, where the first five evolve according to the events

$$(a_1, b_1, s_1, a, b) \underset{w_A^+}{\overset{w_A^-}{\rightleftarrows}} (a_1 - 1, b_1, s_1 + n, a, b) \quad \text{(Equation 45)}$$

$$(a_1, b_1, s_1, a, b) \underset{w_B^+}{\overset{w_B^-}{\rightleftarrows}} (a_1, b_1 - 1, s_1 + n, a, b) \quad \text{(Equation 46)}$$

$$(a_1, b_1, s_1, a, b) \underset{w_S^+}{\overset{w_S^-}{\rightleftarrows}} (a_1, b_1, s_1 - 1, a, b) \quad \text{(Equation 47)}$$

$$(a_1, b_1, s_1, a, b) \underset{w_{A,1}^d}{\overset{w_{A,1}^b}{\rightleftarrows}} (a_1 + 1, b_1, s_1 - n, a + 1, b) \quad \text{(Equation 48)}$$

$$(a_1, b_1, s_1, a, b) \underset{w_{A,2}^d}{\overset{w_{A,2}^b}{\rightleftarrows}} (a_1, b_1, s_1, a + 1, b) \quad \text{(Equation 49)}$$

$$(a_1, b_1, s_1, a, b) \underset{w_{B,1}^d}{\overset{w_{B,1}^b}{\rightleftarrows}} (a_1, b_1 + 1, s_1 - n, a, b + 1) \quad \text{(Equation 50)}$$

$$(a_1, b_1, s_1, a, b) \underset{w_{B,2}^d}{\overset{w_{B,2}^b}{\rightleftarrows}} (a_1, b_1, s_1, a, b + 1), \quad \text{(Equation 51)}$$

with rates as defined above. The statistics of the degrees of freedom can be described by a probability distribution $P(a_1, b_1, s_1, a, b, r_A, r_B, t)$. To study fluctuations in total- and dilute phase volume fractions, we calculated the first- and second-order moments of this probability distribution. Since the system is nonlinear, however, we cannot calculate these moments exactly. Similarly to our

Please cite this article in press as: Zechner and Jülicher, Concentration buffering and noise reduction in non-equilibrium phase-separating systems, Cell Systems (2025), https://doi.org/10.1016/j.cels.2025.101168

previous work,[11] we address this problem by employing the linear noise approximation (LNA),[23] which yields first- and second-order moments consistent with a Gaussian approximation. In general, the LNA becomes accurate for large systems consisting of sufficiently many particles. To apply the LNA to the considered system, we describe both $r_A(t)$ and $r_B(t)$ as birth-and-death processes $\mathcal{BD}(\lambda_1, \lambda_2 r_X(t))$ for $X \in \{A,B\}$, which can be used to represent stochastic mRNA synthesis and turnover,[21] for instance. In this case, the protein synthesis rate $w_X^b = Vk_1^X r_X(t)$ depends on the number of mRNA molecules $r_X(t)$. The corresponding first- and second-order statistics of $r_X(t)$ at stationarity are given by

$$\langle r_X \rangle = \frac{\lambda_1}{\lambda_2} \quad \text{(Equation 52)}$$

$$\mathrm{Var}[r_X] = \frac{\lambda_1}{\lambda_2} = \sigma_X^2 \quad \text{(Equation 53)}$$

$$\kappa_X(\tau) = \sigma_X^2 e^{-\lambda_2 \tau}. \quad \text{(Equation 54)}$$

Ordinary differential equations capturing the time-evolution of the approximate moments were obtained using custom-made code in MATLAB (Version 9.10 (R2021a), The MathWorks Inc., Natick, Massachusetts). Probability distributions over volume fractions were estimated by first sampling copy numbers ($N = 10^6$) from a multivariate normal distribution parameterizied by the moments obtained from the LNA, and subsequently transformed into volume fractions.

Analytical results for the case of a two-component mixture

In the case of a two-component mixture ($\psi = 0$), we obtain approximate closed-form expressions that allow us to study concentration buffering and noise reduction analytically. This approximation considers small ϕ_1 and V_2 and we refer to it as dilute approximation. At equilibrium, the two-component system can be described by the free energy

$$F(a_1, s_1) = v(a_1 n + s_1) f\left(\frac{a_1 n}{a_1 n + s_1}\right) + (V - v(a_1 n + s_1)) f\left(\frac{(a - a_1) n v}{V - v(a_1 n + s_1)}\right) + (36\pi)^{1/3} (V - v(a_1 n + s_1))^{2/3}, \quad \text{(Equation 55)}$$

with

$$f(\phi) = \frac{k_B T}{v}\left[\chi_{AS}\phi(1-\phi) + \frac{\phi}{n}\log\phi + (1-\phi)\log(1-\phi)\right]. \quad \text{(Equation 56)}$$

For simplicity, and because surface tensions tend to be low for biomolecular condensates,[35] we focus on the limit of small surface tension and set $\gamma = 0$ in the following. The system exhibits two kinetic modes driven by the generalized thermodynamic forces that impose conditions on the rates

$$\log \frac{w_A^-(a_1, s_1)}{w_A^+(a_1 - 1, s_1 + n)} = -\frac{nv}{k_B T}\left(\mu_2^A - \mu_1^A\right) \quad \text{(Equation 57)}$$

$$\log \frac{w_S^-(a_1, s_1)}{w_S^+(a_1, s_1 - 1)} = -\frac{v}{k_B T}\left[\Pi_2 - \Pi_1\right], \quad \text{(Equation 58)}$$

where $\mu_\alpha^A = f'(\phi_\alpha)$ and $\Pi_\alpha = f(\phi_\alpha) - \phi_\alpha f'(\phi_\alpha)$. To simplify, we eliminate one of the two degrees of freedom by considering the system to be in osmotic equilibrium, such that $\Pi_1 = \Pi_2$ is satisfied at all times. Expressing $\Pi_1 = \Pi_2$ in terms of ϕ_1 and ϕ_2 yields

$$\frac{(\phi_1 - \phi_2)}{n}(n + n(\phi_1 + \phi_2)\chi_{AS} - 1) + \log(1 - \phi_1) - \log(1 - \phi_2) = 0. \quad \text{(Equation 59)}$$

This equation defines a function $\tilde{\phi}_2 = \omega(\phi_1)$ that describes osmotic equilibrium. Unfortunately, this function cannot be expressed explicitly. We therefore focus on the dilute limit where ϕ_1 is small. Considering only leading order terms, the free energy density in the dilute phase can be approximated as

$$f(\phi_1) \simeq \frac{k_B T}{v}\phi_1(\log \phi_1 - 1 + \chi_{AS}) \quad \text{(Equation 60)}$$

and Equation 59 simplifies to

$$\frac{\phi_1}{n} + \frac{\phi_2}{n}(n + n\phi_2\chi_{AS} - 1) + \log(1 - \phi_2) \simeq 0. \quad \text{(Equation 61)}$$

Please cite this article in press as: Zechner and Jülicher, Concentration buffering and noise reduction in non-equilibrium phase-separating systems, Cell Systems (2025), https://doi.org/10.1016/j.cels.2025.101168

For small ϕ_1, however, the terms independent of ϕ_1 will dominate such that $\tilde{\phi}_2$ can be approximated by solving

$$\frac{\phi_2}{n}(n + n\phi_2\chi_{AS} - 1) + \log(1 - \phi_2) = 0 \quad \text{(Equation 62)}$$

with respect to ϕ_2. As a result of this approximation, dense phase concentrations will be fixed to a value $\tilde{\phi}_2$ that is independent of ϕ_1. Equation 62 is straightforward to solve numerically for a given set of parameters n and χ_{AS}. Once determined, we can express s_1 as a function of a_1 by solving

$$\tilde{\phi}_2 = \frac{(a - a_1)nv}{V - v(a_1 n + s_1)}, \quad \text{(Equation 63)}$$

with respect to s_1, which yields

$$\tilde{s}_1 = \frac{V}{v} - n\frac{a + a_1\left(\tilde{\phi}_2 - 1\right)}{\tilde{\phi}_2}. \quad \text{(Equation 64)}$$

Substituting this expression into the free energy Equation 55 with $f(\phi_1)$ approximated by Equation 60 and $\gamma = 0$ yields

$$F(a_1) = \frac{nv}{\tilde{\phi}_2} f\left(\tilde{\phi}_2\right)(a - a_1) + k_B T a_1 \left[\log\left(\frac{a_1 vn}{V - nv(a - a_1)\Big/\tilde{\phi}_2}\right) - n\right] + k_B T \chi_{AS} a_1 n. \quad \text{(Equation 65)}$$

Defining $\xi = vf\left(\tilde{\phi}_2\right)/\left(k_B T\tilde{\phi}_2\right)$, we can write this more compactly as

$$\begin{aligned}\frac{F(a_1)}{k_B T} &= \xi(a - a_1)n + a_1\left[\log\left(\frac{a_1 nv}{V - nv(a - a_1)\Big/\tilde{\phi}_2}\right) - n\right] + \chi_{AS} a_1 n \\ &= -\mu(a - a_1)n + a_1\left[\log\left(\frac{a_1 nv}{V - nv(a - a_1)\Big/\tilde{\phi}_2}\right) - n\right] + const., \quad \text{(Equation 66)}\end{aligned}$$

with $\mu = \chi_{AS} - \xi$. Note that when $n = 1$ and $\tilde{\phi}_2$, this reduced approximate system becomes equivalent to the binary system analyzed in our previous work.[11] This system can be further simplified in the case where the volume of the dense phase is small compared to the total volume ($V_2 \ll V$). In this case, the mixing entropy in Equation 66 simplifies and we get

$$\frac{F(a_1)}{k_B T} \simeq -\mu(a - a_1)n + a_1\left[\log\left(\frac{a_1 nv}{V}\right) - n\right]. \quad \text{(Equation 67)}$$

Equation 67 is the final form of the free energy that the dilute approximation is based on. Due to the simplifications made, only one kinetic mode remains, associated with the thermodynamic force

$$\begin{aligned}\log\frac{w_A^-(a_1)}{w_A^+(a_1 - 1)} &= \frac{F'(a_1)}{k_B T} \\ &= 1 - n + \mu + \log\left(\frac{a_1 nv}{V}\right).\end{aligned} \quad \text{(Equation 68)}$$

This force is zero when

$$a_{sat} = \frac{V}{nv} e^{-1+n-\mu} \quad \text{(Equation 69)}$$

or equivalently

$$\phi_{sat} = e^{-1+n-\mu}, \quad \text{(Equation 70)}$$

where we refer to a_{sat} and ϕ_{sat} as saturation copy number and saturation concentration, respectively. This terminology reflects the fact that once the total volume fraction ϕ exceeds ϕ_{sat}, the average dilute phase volume fraction $\langle\phi_1\rangle$ remains constant at ϕ_{sat}. The volume fraction ϕ_{sat} thus marks the threshold above which the mixture is saturated and phase coexistence is favorabe.

In the small droplet limit, we can use Equation 68 to express the partitioning rates as

$$w_A^-(a_1) = k_D a_1 \quad \text{(Equation 71)}$$

Please cite this article in press as: Zechner and Jülicher, Concentration buffering and noise reduction in non-equilibrium phase-separating systems, Cell Systems (2025), https://doi.org/10.1016/j.cels.2025.101168

$$w_A^+(a_1 - 1) = w_A^-(a_1)e^{-\frac{F'(a_1)}{k_BT}} = k_D\frac{V}{nv}e^{1-n-\mu} = k_D a_{sat}, \quad \text{(Equation 72)}$$

where we have used $k_D = 6D/V^{2/3}$. In the considered regime, the exchange of solutes from the dilute phase to the dense phase is approximately linear, while the corresponding reverse rate becomes constant. In combination with solute synthesis and turnover, this system has degrees of freedom (a_1, a), which evolve according to the events

$$(a_1, a) \underset{w_A^+}{\overset{w_A^-}{\rightleftarrows}} (a_1 - 1, a) \quad \text{(Equation 73)}$$

$$(a_1, a) \underset{w_{A,1}^d}{\overset{w_{A,1}^b}{\rightleftarrows}} (a_1 + 1, a + 1) \quad \text{(Equation 74)}$$

$$(a_1, a) \underset{w_{A,2}^d}{\overset{w_{A,2}^b}{\rightleftarrows}} (a_1, a + 1). \quad \text{(Equation 75)}$$

Consistent with the small droplet limit, the synthesis rates in the dilute- and dense phase become $w_{A,1}^b(a_1, a) = Vk_1^A r_A(t)$ and $w_{A,2}^b(a_1, a) = 0$, which means that solute synthesis in the dense phase becomes negligible. The turnover rates are given by $w_{A,1}^d(a_1, a) = k_2 a_1(t)$ and $w_{A,2}^d(a_1, a) = k_2(a(t) - a_1(t))$. Notice that because the rate w_A^+ is independent of $a(t)$, we can describe $a_1(t)$ in isolation by the effective birth-and-death process

$$a_1 \underset{Vk_1^A r_A(t) + k_D a_{sat}}{\overset{(k_2+k_D)a_1}{\rightleftarrows}} a_1 - 1, \quad \text{(Equation 76)}$$

or equivalently, $a_1(t) \sim \mathcal{BD}(Vk_1^A r_A(t) + k_D a_{sat}, (k_2 + k_D)a_1(t))$. Here we have made use of the fact that two event channels with the same stoichiometric change can be summarized into a single one with their respective rates added. Using an analogous derivation as for the generic birth-and-death process in STAR Methods section "Accounting for non-equilibrium production and turnover of solutes," we can write down the average solute copy number and noise strength at stationarity as

$$\langle a_1 \rangle = \frac{Vk_1^A\langle r_A\rangle + k_D a_{sat}}{k_2 + k_D} = \frac{k_D}{k_2 + k_D}a_{sat} + \frac{k_2}{k_2 + k_D}\langle a\rangle \quad \text{(Equation 77)}$$

$$\begin{aligned}\eta^2[a_1] &= \frac{k_2 + k_D}{Vk_1^A\langle r_A\rangle + k_D a_{sat}} + \left(\frac{Vk_1^A}{Vk_1^A\langle r_A\rangle + k_D a_{sat}}\right)^2 [k_2 + k_D]\widehat{\kappa}_A(k_2 + k_D) \\ &= \frac{1}{\langle a_1\rangle} + \frac{1}{k_2 + k_D}\left(\frac{Vk_1^A}{\langle a_1\rangle}\right)^2 \widehat{\kappa}_A(k_2 + k_D)\end{aligned} \quad \text{(Equation 78)}$$

Since $V_1 \to V$ in the limit of small droplets, the volume fraction ϕ_1 is just a_1 times a constant, such that the statistics of $\langle\phi_1\rangle$ are readily obtained as

$$\langle\phi_1\rangle = \frac{k_D}{k_2 + k_D}\phi_{sat} + \frac{k_2}{k_2 + k_D}\langle\phi\rangle \quad \text{(Equation 79)}$$

$$\eta^2[\phi_1] = \frac{nv}{V}\frac{1}{\langle\phi_1\rangle} + \frac{1}{k_2 + k_D}\left(\frac{k_1^A nv}{\langle\phi_1\rangle}\right)^2 \widehat{\kappa}_A(k_2 + k_D), \quad \text{(Equation 80)}$$

where Equation 80 is identical to Equation 78 but expressed in terms of $\langle\phi_1\rangle$ instead of $\langle a_1\rangle$. Based on Equation 79, we can further define the apparent partition coefficient

$$\rho = \frac{\langle\phi_2\rangle}{\langle\phi_1\rangle} \simeq \frac{\tilde{\phi}_2}{\langle\phi_1\rangle} = \frac{\tilde{\phi}_2(1 + k_D/k_2)}{\phi_{sat}k_D/k_2 + \langle\phi\rangle}, \quad \text{(Equation 81)}$$

which decreases with $\langle\phi_1\rangle$ and $\langle\phi\rangle$.

Noise reduction in the limit of large volumes and quasi-static birth-rates

Based on the dilute approximation, noise reduction in the binary system is given by

Please cite this article in press as: Zechner and Jülicher, Concentration buffering and noise reduction in non-equilibrium phase-separating systems, Cell Systems (2025), https://doi.org/10.1016/j.cels.2025.101168

$$\Gamma = \frac{\eta[\phi]}{\eta[\phi_1]} \simeq \sqrt{\frac{\frac{nv}{V}\frac{1}{\langle\phi\rangle}+\frac{1}{k_2}\left(\frac{k_1^A nv}{\langle\phi\rangle}\right)^2 \widehat{\kappa}_A(k_2)}{\frac{nv}{V}\frac{1}{\langle\phi_1\rangle}+\frac{1}{k_2+k_D}\left(\frac{k_1^A nv}{\langle\phi_1\rangle}\right)^2 \widehat{\kappa}_A(k_2+k_D)}}. \quad \text{(Equation 82)}$$

To study how this relationship changes for macroscopic systems where intrinsic fluctuations of solute synthesis, turnover and partitioning become small, we take the large volume limit while keeping the diffusion rate k_D constant. Fluctuations in the birth-rate $r_A(t)$ are considered to be independent of volume such that its stationary mean $\langle r_A\rangle$ and autocovariance function $\kappa_A(\tau)$ remain unaffected by volume scaling. If we now let $V\to\infty$, Equation 82 becomes

$$\begin{aligned}\lim_{V\to\infty}\Gamma &= \frac{\langle\phi_1\rangle}{\langle\phi\rangle}\sqrt{\frac{k_2+k_D}{k_2}\frac{\widehat{\kappa}_A(k_2)}{\widehat{\kappa}_A(k_2+k_D)}} \\ &= \underbrace{\left[1+\frac{k_D}{k_2}\frac{\phi_{sat}}{\langle\phi\rangle}\right]}_{=\Lambda}\sqrt{\frac{k_2}{k_2+k_D}\frac{\widehat{\kappa}_A(k_2)}{\widehat{\kappa}_A(k_2+k_D)}},\end{aligned} \quad \text{(Equation 83)}$$

where the first term in the second line is the buffering strength

$$\Lambda = \left|\frac{\mathrm{d}\log\langle\phi_1\rangle}{\mathrm{d}\log\langle\phi\rangle}\right|^{-1} = 1+\frac{k_D}{k_2}\frac{\phi_{sat}}{\langle\phi\rangle} \quad \text{(Equation 84)}$$

calculated using the concentration dependency Equation 79. Thus, noise reduction in the macroscopic limit can be approximated by the buffering strength multiplied by a factor, which depends on the autocovariance function κ_A (or its Laplace transform $\widehat{\kappa}_A$) and the parameters k_2 and k_D. Due to this factor, the noise reduction Γ and the buffering strength Λ can be substantially different, as reflected by our results in the main text. In the limit where fluctuations in $r_A(t)$ decay infinitely slowly, we have $\kappa_A(\tau)=\sigma_A^2$ with σ_A as the standard deviation of $r_A(t)$. The corresponding Laplace transform becomes $\widehat{\kappa}_A(u)=\sigma_A^2 u^{-1}$. Only in this special case, the second factor in Equation 83 becomes equal to one such that noise reduction becomes equal to the buffering strength.

We remark that the analysis above focuses on noise reduction and concentration buffering within the dilute approximation, where the system dynamics are linear. For non-linear systems, equivalence between noise reduction and the buffering strength in the limit of large volumes and quasi-static fluctuations $r_A(t)$ can be established only approximately. To see this, consider a system at a non-equilibrium steady state with total- and dilute phase concentration ϕ and ϕ_1. The dynamics of ϕ and ϕ_1 are affected by a stationary stochastic process $r_A(t)$. The system is such that in the large volume limit ($V\to\infty$), intrinsic fluctuations in ϕ and ϕ_1 vanish. In this limit, all fluctuations in ϕ and ϕ_1 are due to fluctuations in $r_A(t)$. If we further consider the case where $r_A(t)$ fluctuates very slowly on the timescale of ϕ and ϕ_1, we can express the relationship between ϕ and ϕ_1 as a function $\phi_1=\zeta(\phi(r_A))$, where r_A is a constant random variable. When variations in r_A are small, we have approximately

$$\phi \simeq \phi(\langle r_A\rangle)+\phi'(\langle r_A\rangle)(r_A-\langle r_A\rangle) \quad \text{(Equation 85)}$$

$$\phi_1 \simeq \zeta(\phi(\langle r_A\rangle))+\phi'(\langle r_A\rangle)\zeta'(\phi(\langle r_A\rangle))(r_A-\langle r_A\rangle). \quad \text{(Equation 86)}$$

Averaging over r_A yields for the concentration dependency

$$\langle\phi_1\rangle = g_{NE}(\langle\phi\rangle)\simeq\zeta(\phi(\langle r_A\rangle)). \quad \text{(Equation 87)}$$

For the standard deviation of ϕ and ϕ_1 we obtain

$$\sigma[\phi]\simeq\sigma_r|\phi'(\langle r_A\rangle)| \quad \text{(Equation 88)}$$

$$\sigma[\phi_1]\simeq\sigma_r|\phi'(\langle r_A\rangle)||\zeta'(\phi(\langle r_A\rangle))| = \sigma[\phi]|\zeta'(\phi(\langle r_A\rangle))| \quad \text{(Equation 89)}$$

with σ_r as the standard deviation of r_A. The noise reduction Γ can thus be approximated as

$$\Gamma\simeq\frac{1}{\phi(\langle r_A\rangle)}\frac{\zeta(\phi(\langle r_A\rangle))}{|\zeta'(\phi(\langle r_A\rangle))|}. \quad \text{(Equation 90)}$$

The buffering strength, is calculated as

$$\Lambda = \left|\frac{\mathrm{d}\log(\langle\phi_1\rangle)}{\mathrm{d}\log(\langle\phi\rangle)}\right|^{-1}\simeq\frac{1}{\phi(\langle r_A\rangle)}\frac{\zeta(\phi(\langle r_A\rangle))}{|\zeta'(\phi(\langle r_A\rangle))|}, \quad \text{(Equation 91)}$$

Please cite this article in press as: Zechner and Jülicher, Concentration buffering and noise reduction in non-equilibrium phase-separating systems, Cell Systems (2025), https://doi.org/10.1016/j.cels.2025.101168

which is identical to the approximate expression for noise reduction Γ in Equation 90. In this more general case, the noise reduction Γ and the buffering strength Λ are thus expected to become similar only in the limit where the system size V is very large, the correlation time of the upstream fluctuations $r_A(t)$ diverges and additionally, variations in $r_A(t)$ are small. Beyond this limit, these two quantities provide different insights and cannot be exchanged.

Example

To further illustrate the difference between concentration buffering and noise reduction, we analyze Equation 83 in the context of a simple example. In particular, we choose $\kappa_A(\tau) = \sigma_A^2 e^{-\lambda_2 \tau}$, corresponding to a stochastic process with a correlation time λ_2^{-1}. The Laplace transform of κ_A is

$$\widehat{\kappa}_A(u) = \frac{\sigma_A^2}{u+\lambda_2} \tag{Equation 92}$$

and correspondingly, Equation 83 becomes

$$\Gamma = \left[1 + \frac{k_D}{k_2}\frac{\phi_{sat}}{\langle\phi\rangle}\right]\sqrt{\frac{k_2}{k_2+k_D}\frac{k_2+k_D+\lambda_2}{k_2+\lambda_2}}. \tag{Equation 93}$$

As can be seen, noise reduction becomes identical to the buffering strength (Equation 84) only as $\lambda_2 \to 0$.

QUANTIFICATION AND STATISTICAL ANALYSIS

Synthetic system

We analyzed experimental concentration measurements from the 2NT-DDX4^{YFP} that we published previously using the theory outlined here.[11] In particular, we focussed on two datasets, one where dilute- and total concentrations c_1 and c were measured for a large number of cells (Figure 2c in Klosin et al.[11]), and one for which dilute- and dense phase concentrations c_1 and c_2 were measured for a smaller number of cells (Figure S22 in Klosin et al.[11]). We used the former one to estimate timescale ratios using the calculated concentration dependency under the dilute approximation (Equation 79). To do so, we first estimated the relationship between $\langle c_1\rangle$ and $\langle c\rangle$ from the experimental measurements. To select cells well within the regime of phase coexistence, we excluded cells that had a total concentration below 12 μM. We divided the remaining measurements of total concentrations into K non-overlapping intervals. The lower- and upper limit of the k th interval were determined as $l_k = q(k/K)$ and $u_k = q((k+1)/K)$ where $k = 0, \ldots, K-1$ and $q(x)$ is the empirical x-quantile of the experimentally measured sample of total concentrations. As an example, $q(0.5)$ would correspond to the median total concentration. The rationale behind using (equally-spaced) quantiles as the interval boundaries is that we obtain an approximately equal number of samples in each interval. Average total- and dilute phase concentrations for interval k, $\overline{c}^{(k)}$ and $\overline{c}_1^{(k)}$, were estimated using all cells i for which $l_k < c^{(i)} \leq u_k$, where $c^{(i)}$ is the measured total concentration for cell i. The corresponding uncertainties of $\overline{c}^{(k)}$ and $\overline{c}_1^{(k)}$ were determined using bootstrapping.[36] Assuming that the number of samples in each interval is sufficiently large, we can make use of the central limit theorem and describe $(\overline{c}^{(k)}, \overline{c}_1^{(k)})^T$ as a Gaussian random vector such that

$$\begin{pmatrix}\overline{c}^{(k)}\\ \overline{c}_1^{(k)}\end{pmatrix} = \begin{pmatrix}\langle c\rangle\\ \langle c_1\rangle\end{pmatrix} + \begin{pmatrix}\Delta^{(k)}\\ \Delta_1^{(k)}\end{pmatrix} \quad \text{with} \quad \begin{pmatrix}\Delta^{(k)}\\ \Delta_1^{(k)}\end{pmatrix} \sim N(0, \Sigma^{(k)}) \quad \text{and} \quad \Sigma^{(k)} = \begin{pmatrix}\Sigma_{11}^{(k)} & \Sigma_{12}^{(k)}\\ \Sigma_{12}^{(k)} & \Sigma_{22}^{(k)}\end{pmatrix}, \tag{Equation 94}$$

where $\Sigma^{(k)}$ are the empirical uncertainties of $(\overline{c}^{(k)}, \overline{c}_1^{(k)})^T$ obtained via bootstrapping. Reformulating Equation 79 in terms of concentrations (as opposed to volume fractions) and expressing $\langle c\rangle$ and $\langle c_1\rangle$ in terms of experimentally determined quantities $\overline{c}^{(k)}$ and $\overline{c}_1^{(k)}$ yields

$$\begin{aligned}\overline{c}_1^{(k)} &= \frac{k_D}{k_2+k_D}c_{sat} + \frac{k_2}{k_2+k_D}\overline{c}^{(k)} - \frac{k_2}{k_2+k_D}\Delta^{(k)} + \Delta_1^{(k)}\\ &= \frac{k_D}{k_2+k_D}c_{sat} + \frac{k_2}{k_2+k_D}\overline{c}^{(k)} + \bar{\Delta}^{(k)},\end{aligned} \tag{Equation 95}$$

with $c_{sat} = \phi_{sat}/(nv)$ and $\bar{\Delta}^{(k)} = \Delta_1^{(k)} - k_2/(k_2+k_D)\Delta^{(k)}$. Since $\bar{\Delta}^{(k)}$ is a linear combination of two Gaussians, it is itself a Gaussian, i.e., $\bar{\Delta}^{(k)} \sim N(0, \overline{\Sigma}^{(k)})$, with

$$\begin{aligned}\overline{\Sigma}^{(k)} &= \begin{pmatrix}-\frac{k_2}{k_2+k_D} & 1\end{pmatrix}\begin{pmatrix}\Sigma_{11}^{(k)} & \Sigma_{12}^{(k)}\\ \Sigma_{12}^{(k)} & \Sigma_{22}^{(k)}\end{pmatrix}\begin{pmatrix}-\frac{k_2}{k_2+k_D}\\ 1\end{pmatrix}\\ &= \frac{k_2^2}{(k_2+k_D)^2}\Sigma_{11}^{(k)} + \Sigma_{22}^{(k)} - 2\frac{k_2}{k_2+k_D}\Sigma_{12}^{(k)}.\end{aligned} \tag{Equation 96}$$

Please cite this article in press as: Zechner and Jülicher, Concentration buffering and noise reduction in non-equilibrium phase-separating systems, Cell Systems (2025), https://doi.org/10.1016/j.cels.2025.101168

Thus, fitting the analytical concentration dependency to the experimentally determined one is a regression problem with parameter-dependent errors. Note that with k_2, k_D and c_{sat}, the model is overparameterized and thus, not all parameters can be determined uniquely. However, we can reparameterize the model in terms of k_D/k_2 and c_{sat} and thereby eliminate one unknown degree of freedom. The resulting two parameters and their uncertainties can be inferred using Bayes' rule, which reads

$$p\left(k_D/k_2, c_{sat} \,\middle|\, \left(\overline{c}^{(0)}, \overline{c}_1^{(0)}\right), \ldots, \left(\overline{c}^{(K-1)}, \overline{c}_1^{(K-1)}\right)\right) \propto p(k_D/k_2, c_{sat}) \prod_{k=0}^{K-1} N\left(\overline{c}_1^{(k)} - \frac{k_D}{k_2+k_D} c_{sat} - \frac{k_2}{k_2+k_D}\overline{c}^{(k)} \,\middle|\, 0, \overline{\Sigma}^{(k)}\right), \quad \text{(Equation 97)}$$

where we consider the prior distribution $p(k_D/k_2, c_{sat})$ to be flat in the log-domain. Posterior distributions where sampled over logarithmic parameters (i.e., $\log k_D/k_2$ and $\log c_{sat}$) using the Metropolis-Hastings algorithm.[37] The proposal distribution was chosen to be a bivariate normal distribution such that $x^* \sim N(x, \sigma_p^2 \mathbb{I}_2)$ with x and x^* as the current and proposed parameters, respectively and $\mathbb{I}_2$ as the 2×2 identity matrix. The standard deviation σ_p was chosen to be 0.1. The chain was simulated for $M = 10^5$ steps and the first 10^4 samples were discarded to eliminate the initial burn-in period of the chain. Minimum mean squared error (MMSE) estimates were determined by calculating the component-wise mean of the resulting samples. Corresponding uncertainties were estimated as the component-wise standard deviations. When choosing the number of intervals to be $K = 34$, we estimated $c_{sat} = (7.471 \pm 0.053)\ \mu$M and $k_D/k_2 = 21.569 \pm 1.426$. Doubling the number of intervals to $K = 68$ only marginally affected the inferred parameters ($c_{sat} = (7.494 \pm 0.050)\ \mu M$ and $k_D/k_2 = 22.560 \pm 1.4252$), showing that the results are robust for varying K.

We further analyzed partition coefficients in the 2NT-DDX4^{YFP} system using the data from Figure S22 in Klosin et al.[11] Rewriting Equation 81 in terms of concentrations yields for the apparent partition coefficient

$$\rho = \frac{\langle c_2 \rangle}{\langle c_1 \rangle} \simeq \frac{\tilde{c}_2(1+k_D/k_2)}{c_{sat}k_D/k_2+\langle c \rangle}, \quad \text{(Equation 98)}$$

where $\langle c_2 \rangle \simeq \tilde{c}_2 = \tilde{\phi}_2/(nv)$ under the dilute approximation. Thus, the partition coefficient is expected to decrease with average total (and thus, dilute phase-) concentration as long as k_D/k_2 is finite. As $k_D/k_2 \to \infty$, the partition coefficient becomes $\tilde{c}_2/c_{sat} = const.$ as the system approaches (quasi-)equilibrium. To compare these predictions to experiments, we calculated partition coefficients c_2/c_1 in individual cells. Since total concentrations were not quantified in this particular dataset, we plotted c_2/c_1 over c_1 as was done also in Riback et al.[7] The resulting data is compared to the apparent partition coefficient $\rho = \tilde{c}_2/\langle c_1 \rangle$, where $\tilde{c}_2$ was determined as the average dense phase concentration calculated over individual cells (Figure S22 in Klosin et al.[11]).

Endogenous system

The data in Figure S2B shows dilute- over total concentrations of fluorescently labelled NPM1 from two previously published studies.[7,11] The first one corresponds to endogenously labelled NPM1 (Figure 3F in Klosin et al.[11]). Total concentrations c were measured during mitosis, when the nucleolus is dissolved. Dilute phase concentrations c_1 were measured ten hours later during interphase, when the nucleolus coexists with nucleoplasmic NPM1. Note that since c and c_1 were measured at different time points, the resulting relationship between c and c_1 is approximate. However, it nevertheless allows us to study concentration variability in the presence and absence of the nucleolus. To approximately convert fluorescence intensities to molar concentrations, we rescaled intensity values to achieve a mean total concentration of 7.7 μM as measured previously.[38] The second dataset was obtained from Riback et al.,[7] where fluorescently labelled NPM1 was overexpressed on top of native, unlabelled NPM1 (Figure 1b in Riback et al.[7]). These data were replotted as originally published and shown together with the calibrated, endogenous NPM1 measurements from our previous study[11] in Figure S2B.